Endocytosis of Hedgehog through Dispatched Regulates Long-Range Signaling

Gisela d'Angelo, Tamás Matusek, Sandrine Pizette, Pascal p. Thérond

▶ **To cite this version:**

Gisela d'Angelo, Tamás Matusek, Sandrine Pizette, Pascal p. Thérond. Endocytosis of Hedgehog through Dispatched Regulates Long-Range Signaling. Developmental Cell, 2015, 32 (3), pp.290-303. 10.1016/j.devcel.2014.12.004 . hal-03033949

HAL Id: hal-03033949
https://hal.science/hal-03033949v1

Submitted on 9 Dec 2021

HAL is a multi-disciplinary open access archive for the deposit and dissemination of scientific research documents, whether they are published or not. The documents may come from teaching and research institutions in France or abroad, or from public or private research centers.

L'archive ouverte pluridisciplinaire **HAL**, est destinée au dépôt et à la diffusion de documents scientifiques de niveau recherche, publiés ou non, émanant des établissements d'enseignement et de recherche français ou étrangers, des laboratoires publics ou privés.

Article

Developmental Cell

Endocytosis of Hedgehog through Dispatched Regulates Long-Range Signaling

Graphical Abstract

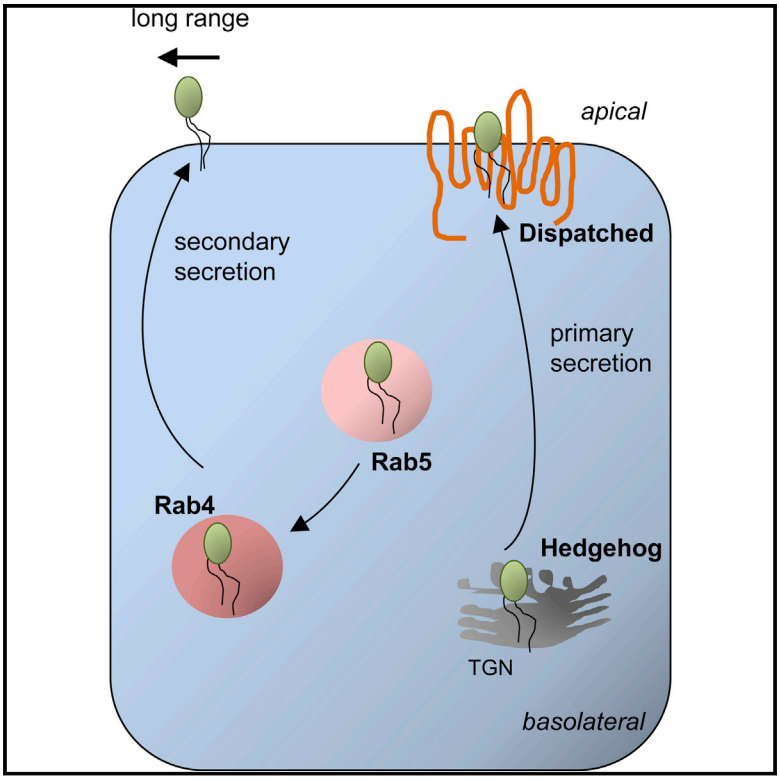

Highlights

- Dispatched is required for the apical endocytosis of Hh in producing cells
- Re-internalized Hh is regulated by Rab5 and Rab4 activity
- Internalization and recycling contribute to regulate Hh long-range activity

Authors

Gisela D'Angelo, Tamás Matusek, Sandrine Pizette, Pascal P. Thérond

Correspondence

dangelo@unice.fr (G.D.),
therond@unice.fr (P.P.T.)

In Brief

D'Angelo et al. examined the relevance of ligand re-internalization in producing cells on the establishment of the Hedgehog morphogen gradient. They demonstrate that Dispatched-mediated apical endocytosis of Hedgehog and its subsequent recycling in a Rab5- and Rab4-dependent manner are two instrumental mechanisms promoting Hedgehog long-range activity.

D'Angelo et al., 2015, Developmental Cell *32*, 290–303
February 9, 2015 ©2015 Elsevier Inc.
http://dx.doi.org/10.1016/j.devcel.2014.12.004

CellPress

Developmental Cell
Article

Endocytosis of Hedgehog through Dispatched Regulates Long-Range Signaling

Gisela D'Angelo,[1,*] Tamás Matusek,[1] Sandrine Pizette,[1] and Pascal P. Thérond[1,*]
[1]Institut de Biologie de Valrose – iBV, Centre de Biochimie, Université Nice Sophia Antipolis, CNRS UMR7277, INSERM 1091, Parc Valrose, 06108 Nice Cedex 2, France
*Correspondence: dangelo@unice.fr (G.D.), therond@unice.fr (P.P.T.)
http://dx.doi.org/10.1016/j.devcel.2014.12.004

SUMMARY

The proteins of the Hedgehog (Hh) family are secreted proteins exerting short- and long-range control over various cell fates in developmental patterning. The Hh gradient in *Drosophila* wing imaginal discs consists of apical and basolateral secreted pools, but the mechanisms governing the overall establishment of the gradient remain unclear. We investigated the relative contributions of endocytosis and recycling to control the Hh gradient. We show that, upon its initial apical secretion, Hh is re-internalized. We examined the effect of the resistance-nodulation-division transporter Dispatched (Disp) on long-range Hh signaling and unexpectedly found that Disp is specifically required for apical endocytosis of Hh. Re-internalized Hh is then regulated in a Rab5- and Rab4-dependent manner to ensure its long-range activity. We propose that Hh-producing cells integrate endocytosis and recycling as two instrumental mechanisms contributing to regulate the long-range activity of Hh.

INTRODUCTION

The mechanisms by which morphogen gradients are established have been the focus of many investigations. They are thought to involve regulations in the amounts of ligand released, transport across developing tissues, rates of capture, endocytosis, and degradation in receiving cells (Rogers and Schier, 2011).

One of the morphogens for which secretion and transport mechanisms are intensively studied is the Hedgehog (Hh) protein (Briscoe and Thérond, 2013). The processing of the full-length Hh protein (Hh-FL) is atypical because, after signal sequence cleavage, it undergoes autoproteolytic cleavage to generate an amino-terminal peptide that is linked to cholesterol at its carboxyl terminus (Hh-Np). All signaling activities are mediated by Hh-Np, which is further modified by the covalent addition of palmitate, that greatly increases the activity of the protein in cell-based assays (Buglino and Resh, 2008; Mann and Beachy, 2004; Pepinsky et al., 1998; Taylor et al., 2001).

The analysis of the Hh gradient activity in the *Drosophila* wing imaginal disc revealed some key features of its regulation. In the wing disc epithelium, Hh is secreted from the posterior producing cells, which display no transcriptional response to Hh, and it signals in the anterior receiving cells in a concentration gradient-dependent manner. At short-range, the highest levels of Hh at the anterior-posterior (A/P) border turn on expression of genes encoding Engrailed (En) and Patched (Ptc), one of the Hh receptors. At long range, lower levels of Hh are sufficient to induce the expression of the *decapentaplegic* gene (*dpp*), a member of the bone morphogenetic protein (BMP) family, and to stabilize the levels of Cubitus interuptus (Ci), the transcriptional mediator of the pathway (Briscoe and Thérond, 2013). We and others have previously suggested that the Hh gradient is a composite of pools secreted by different routes, apical and basolateral (Ayers et al., 2010; Callejo et al., 2011). Furthermore, we have provided genetic evidence that the Hh pool secreted by the apical pole of Hh-producing cells exerts its long-range effects on low-threshold targets (Ayers et al., 2010).

The long-range Hh activity in the wing imaginal disc raises critical questions as to how a dually lipidated protein escapes from the lipid bilayer of the plasma membrane of producing cells and how it can elicit direct responses at a distance of 10 to 15 cell diameters from the source of production (~50 μm in wing imaginal discs). Several modes of transport involving the shielding of the lipid anchors to allow Hh to be transported extracellularly have been proposed. For example, the long-range activity of Hh has been shown to be dependent on the oligomerization of the protein at the cell surface (Vyas et al., 2008) and soluble cholesterol-modified multimers of Hh have been identified biochemically (Gallet et al., 2006; Zeng et al., 2001). Hh has also been shown to be associated with soluble lipoprotein particles (Panáková et al., 2005) or loaded onto secreted exovesicles in vitro and in vivo (Gradilla et al., 2014; Matusek et al. 2014; Tanaka et al., 2005; Vyas et al. 2014). Furthermore, it has been suggested that Hh spreads on filopodia-like cellular extensions called cytonemes (Bischoff et al., 2013). Improvements in our understanding of the regulation of Hh trafficking in Hh-producing cells should shed light on the mechanisms of Hh release and transportation.

Some insight into the process of Hh release came from the identification of the *dispatched* (*disp*) gene encoding a multipass transmembrane protein of the RND transporter family (Goldberg et al., 1999). Disp contains a sterol-sensing domain (SSD), a sequence of five consecutive membrane-spanning helices found in several membrane proteins involved in cholesterol homeostasis (Kuwabara and Labouesse, 2002), and is involved in the release and long-range activity of the lipid-modified Hh protein from producing cells in fly, mouse, zebrafish, and humans (Burke et al., 1999; Caspary et al., 2002; Kawakami et al., 2002;

CrossMark

Ma et al., 2002; Nakano et al., 2004; Roessler et al., 2009; Tian et al., 2005). Interestingly, a lack of Disp has no effect on intrinsic Hh activity, because expression of the short-range target gene patched (*ptc)* is observed in *disp* mutant tissues (Burke et al., 1999). The vertebrate homolog, DispA, has recently been shown to interact with the cholesterol moiety of human Shh and to act in synergy with the vertebrate-specific Scube2, a secreted glycoprotein that binds to a different part of the cholesterol molecule to promote the release of Shh from the cell surface (Creanga et al., 2012; Tukachinsky et al., 2012). Independently, in *Drosophila* embryonic epithelial cells, Disp has been shown to be required for the apico-basal trafficking of Hh (Gallet et al., 2003).

The mechanism by which Disp promotes long-range Hh signaling remains elusive. Disp is required for Hh secretion, but it remains unclear at which step of Hh secretion Disp is needed within the epithelium. We show here that the trafficking of Hh to the apical pole of producing cells is not affected by Disp. We found that, following its plasma membrane localization, Hh is internalized in Hh-producing cells but is not degraded. Surprisingly, the endocytosis of apical Hh is specifically impaired in the absence of Disp activity, whereas internalization of the general endocytic markers FM4-64 and Dextran is not affected. We also demonstrated that the endocytosis and recycling of Hh in a Rab5- and Rab4-dependent manner was required for its long-range activity. We propose that in addition to its role in the release of Hh from producing cells, Disp also regulates apical internalization and the subsequent recycling of Hh in producing cells, a process necessary to promote the long-range activity of Hh.

RESULTS

Hh Is Internalized in Hh-Producing Cells

To investigate the uptake of Hh in producing cells, we analyzed the distribution of endogenous Hh and GFP-Rab5 expressed at a physiological level from a functional knockin construct (Figures 1A–1B′; Fabrowski et al., 2013). The small GTPase Rab5 localizes to early endosomes and is critical for the fusion of clathrin-coated vesicles with early endosomes (Wandinger-Ness and Zerial, 2014). To disrupt endocytosis, we made use of a constitutively active form of Rab5 blocked in the GTP-bound state (YFP-Rab5^{CA}) and assayed for colocalization with the lipophilic endocytic marker FM4-64. FM4-64 binds to the plasma membrane lipids, is internalized in vesicles that rapidly fuse with early endosomes, and follows the endocytic pathway in a time-dependent manner (Vida and Emr, 1995). In cells expressing YFP-Rab5^{CA}, FM4-64 accumulated in Rab5^{CA}-positive apical endocytic vesicles, suggestive of endocytic defects (Figures S1A–S1B′ available online). Random clones of cells expressing YFP-Rab5^{CA} were induced (Figures 1C–1D′) and the subcellular distribution of Rab5 was compared to the endogenous one. Both GFP-Rab5 and YFP-Rab5^{CA} accumulated at the subapical plane of epithelial cells, below the level of cortical F-actin and E-cadherin (E-cad; Figures 1B and 1D). Endogenous Rab5 distribution was also confirmed with an anti-Rab-5 antibody (Figure 1E). Interestingly endogenous Hh colocalized with GFP-Rab5 and accumulated within Rab5^{CA}-positive apical endocytic vesicles (Figures 1B and 1D, arrows). Note that we did not find accumulation of Hh in cells that overexpressed a WT version of Rab5 (Figures S1C and S1C′).

We also made use of the Hh-GFP fusion protein, which can substitute for the endogenous Hh function (Torroja et al., 2004; Figures S1D–S1G). Hh-GFP expression was driven by the *hhGal4* driver in the posterior compartment and colocalization of Hh-GFP with endogenous Rab5 was analyzed (Figures 1E–1F′). Hh-GFP puncta were found in Rab5-positive endosomes, which were abundant at the apical side of the cells (Figures 1E–1F′).

Taken together, our data show that in posterior cells where Hh is produced, Hh is internalized and trafficked to early endosomes. We also noticed that endogenous Hh or Hh-GFP barely colocalized with Rab5 at the basal plane (Figures 1B, 1D, and 1F).

Cholesterol-Modified Hh-GFP Is Endocytosed from the Apical Surface in Hh-Producing Cells

We wondered whether the internalization of Hh by producing cells may be a key step in the modulation of Hh release. We analyzed the endocytosis of Hh in posterior cells further by studying the dynamics of Hh-GFP internalization in live wing imaginal discs. Hh-GFP was expressed in the posterior compartment and assayed for colocalization with FM4-64. Pulse-chase experiments revealed that Hh-GFP puncta were co-internalized with FM4-64-labeled vesicles (Figures 2A–2D). The percentage of double-labeled vesicles gradually decreased over time and was closely related to the subcellular distribution of FM4-64 vesicles (Figures 2A–2I). Over shorter periods (5 and 15 min), FM4-64 vesicles were more abundant in the apical half of the disc cells (Figures 2E and 2F), whereas at later time points (30 and 45 min), FM4-64 puncta were detected more basolaterally and appeared to fuse into larger structures reminiscent of late endosomes. Surprisingly, very few vesicles at the basal surface were double-labeled for Hh-GFP and FM4-64, suggesting that Hh-GFP is mostly taken up by apical endocytosis. Note that we could not stain for endogenous Hh as the detergent necessary for tissue permeabilization washes out the FM4-64 dye and is thus not compatible with this protocol.

To determine whether the cholesterol moiety of Hh was required for internalization, we examined the cellular uptake of the Hh variant lacking the cholesterol adduct (Hh-N-GFP) (Gorfinkiel et al., 2005). After expression in posterior cells, Hh-N-GFP was present in the anterior compartment, attesting for secretion (Figures S2B and S2E). However very few Hh-N-GFP puncta colocalized with the FM4-64 marker in posterior cells, suggesting that this construct was poorly internalized, if at all (Figures S2H, S2K, and S2N; Table 1). These results demonstrate that lipid-modified Hh is endocytosed from the apical surface of producing cells and that the cholesterol moiety is required for this process.

To examine whether cholesterol modification on its own was sufficient to promote Hh internalization, we analyzed the behavior of the cholesterol-modified GFP-Hh-C, a fusion protein in which the Hh-N peptide has been replaced by GFP, and therefore contains the residues necessary for cholesterol modification of the GFP peptide (Figure S2). A strong intracellular staining for GFP-Hh-C was observed in posterior expressing cells whereas no GFP signal was detected in anterior cells, suggesting that

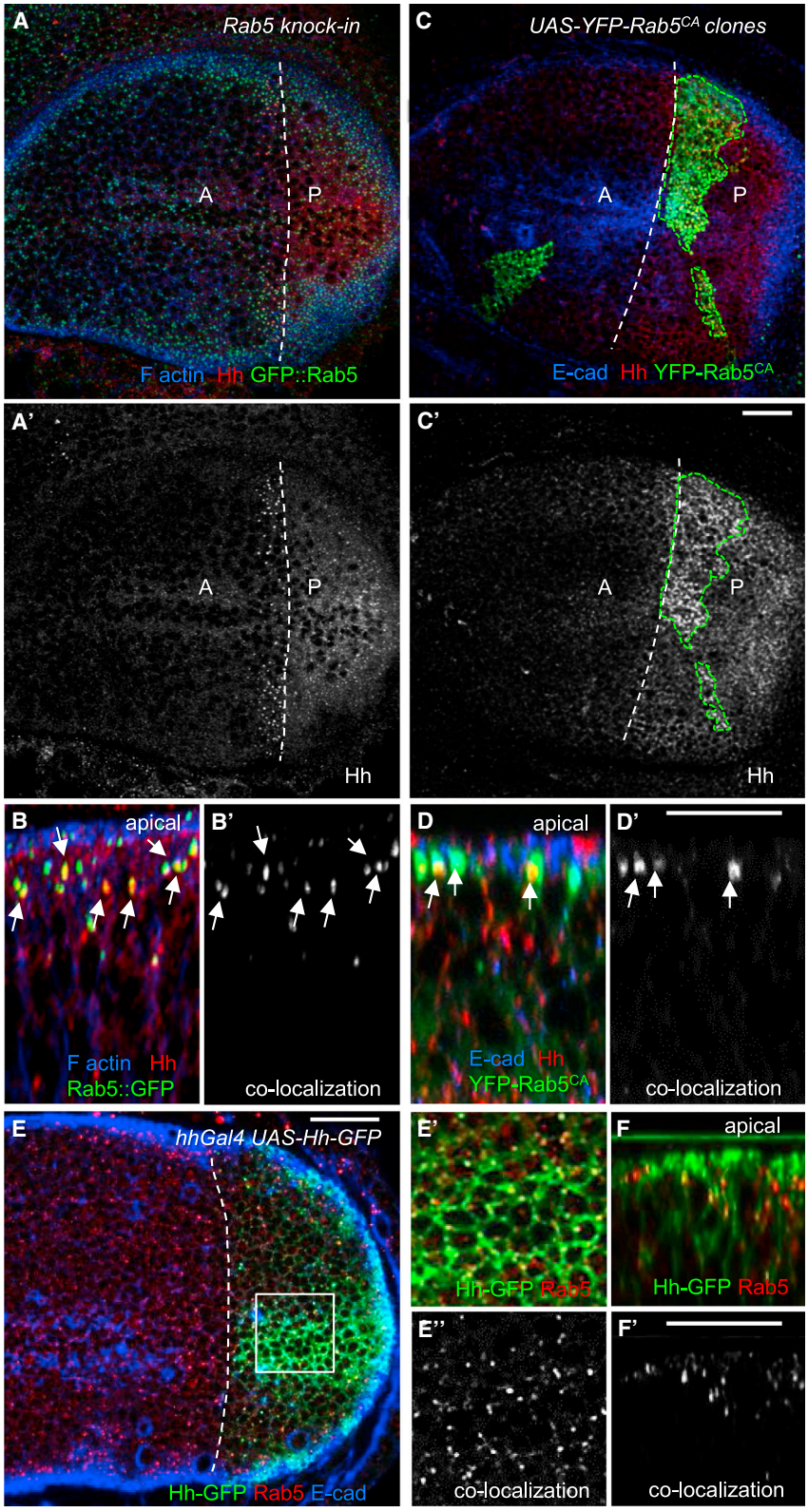

Figure 1. Hh Is Internalized in Rab5-Positive Vesicles in Posterior Cells

(A–B′) Wing imaginal disc expressing Rab5-GFP knockin stained for F-actin (blue), endogenous Hh (red) and Rab5 (green). (A and A′) Single XY sub-apical section and (B and B′) single XZ section through posterior compartment. Endogenous Hh colocalized with GFP-Rab5 below cortical F-actin level. White arrows (B and B′) show examples of colocalization between Hh and endogenous Rab5-positive endosomes.

(C–D′) Wing imaginal disc expressing random ectopic clones of Rab5^{CA}. (C and C′) Projections of four confocal sections 250 nm apart at the apical surface. The overexpression of YFP-Rab5^{CA} protein in a posterior clone caused an increase of Hh levels at the apical surface of Hh-producing cells (red in C, white in C′). The posterior clone is delimited by a green dashed line. (D and D′) Single XZ section perpendicular to the A/P boundary through the posterior Rab5^{CA} clone. E-cad (blue) marks apical junctions. Rab5^{CA}-positive vesicles (green) are apically distributed and (D′) colocalized with endogenous Hh (red), which accumulates in Rab5-positive endosomes. White arrows (D and D′) show examples of colocalization between Hh and Rab5-positive endosomes.

(E–F′) Wing imaginal discs expressing Hh-GFP in the posterior compartment stained with antibodies against GFP (green), Rab5 (red), and E-cad (blue). (E′–E″) High-magnification image of the inset in (E) depicting single confocal section 2 μm below the apical surface. (E′) Anti-GFP and anti-Rab5 staining and (E″) colocalization of both proteins. (F and F′) Single XZ section perpendicular to the D/V axis showing the dual staining for Hh-GFP and Rab5. Note the enrichment of Hh-GFP and Rab5 at the most apical region of the disc. (F′) Only the positive endosomes costained for Rab5 and GFP are shown. In all images, white broken lines delimit the A/P border.

(A–C′) A, anterior compartment; P, posterior compartment.

(C′, D′, F′) Scale bars represent 20 μm. See also Figure S1.

this construct was not secreted (Figures S2C and S2F). Staining for the *cis*-Golgi compartment confirmed that part of GFP-Hh-C accumulated within the Golgi (Figures S2P–S2Q′). We therefore were not able to determine whether the cholesterol modification was sufficient to promote Hh internalization.

Hh Does Not Traffic through the Endocytic Pathway to the Lysosome

The localization of Hh to the endocytic compartment of producing cells suggested the possible trafficking of Hh to the lysosome for degradation. We tested this hypothesis by generating clones of cells mutant for *deep orange* (*dor*), which encodes a homolog of the yeast VPS protein required for the delivery of vesicular cargos to lysosomes (Sevrioukov et al., 1999). The lack of *dor* activity resulted in the accumulation of poly-ubiquitinated epitopes (poly-Ubi) of proteins trafficking to degradative lysosomes (Figures

2L and 2L′). Depletion of *dor* activity in anterior clones close to the A/P border resulted in a 2-fold increase of Hh and Ptc levels (Figures 2J–2J″), probably due to the targeting of Hh/Ptc to the lysosomal compartment as previously shown (Gallet and Therond, 2005; Torroja et al., 2004). In contrast, in posterior *dor* mutant cells, no change in Hh levels was observed, suggesting that Hh, internalized in posterior cells, is not targeted to the degradative pathway (Figures 2K–2L″). We therefore considered the possibility that some of the internalized Hh might be recycled in producing cells.

Rab4 Mediates the Recycling of Hh to the Apical Membrane and Its Long-Range Activity

Previous studies have shown that Rab4 directs fast recycling from early endosomes to the plasma membrane in mammalian cells (de Renzis et al., 2002). We investigated whether recycling played a role in Hh gradient formation by targeting the expression of the dominant-negative protein Rab4 (YFP-Rab4^{DN}) or of RNAi against Rab4 to the dorsal compartment with the *apGal4* driver (Figure 3). Sixteen hours after Rab4^{DN} induction in dorsal cells, apical dorsal Hh staining was decreased by 50% as compared to apical ventral Hh levels (Figures 3A, 3B, and S3E). In dorsal cells, Hh puncta seemed redistributed basolaterally, where they colocalized with the Rab4^{DN}-positive compartment (Figures 3B–3C′). The basolateral redistribution of Hh was specific and was not observed for other markers, such as atypical protein kinase C (aPKC), E-cad, and Disc large (Dlg; Figure S3F). This redistribution was not observed in cells expressing YFP-Rab4^{WT} (Figures S3A–S3C) but was observed in dorsal cells depleted for Rab4 (Figure 3D).

Because the long-range Hh gradient is formed at the apical plane (Ayers et al., 2010), we wondered whether the basolateral redistribution of Hh in Rab4^{DN}- or in Rab4-RNAi- expressing cells would impinge on the long-range activity of Hh in the anterior compartment. Following the expression of YFP-Rab4^{DN} or RNAi against Rab4 in Hh-producing cells, the Hh-dependent stabilization of Ci and *dpp-lacZ* reporter gene expression were significantly reduced, whereas the short-range targets, En and Ptc, were not affected (Figures 3E–3P′). We also found that the overexpression of Rab4-RNAi in the dorsal compartment mimicked the effects of Rab4^{DN} on the long-range activity of Hh, whereas Rab4^{WT} expression had no effect (Figures S3D–S3D″ and S3H–S3K′). Similarly, the expression of Rab5^{DN} in the posterior compartment decreased Hh long-range activity but did not affect the expression of short-range target genes (Figures S3L–S3O).

To test if impaired Hh activity was associated with defects of Hh release, we expressed Rab4^{DN} in the dorsal compartment. This led to an accumulation of Hh at the apical plasma membrane in dorsal-Rab4^{DN} expressing cells compared to their WT neighbors (Figures S3G and S3G′). Accumulated Hh was detected in nonpermeabilized discs (see Experimental Procedures), suggesting that Hh is retained at the outer plasma membrane surface of producing cells.

Altogether, our data suggest that the long-range activity of Hh is promoted by its apical internalization with a major contribution from the canonical Rab5/Rab4-dependent recycling pathway.

Disp Is Not Required for the Trafficking of Hh to the External Surface of Secreting Cells

Given that previous studies have shown that the long-range activity of Hh relies on Disp function (Burke et al., 1999; Caspary et al., 2002; Kawakami et al., 2002; Ma et al., 2002; Nakano et al., 2004; Roessler et al., 2009; Tian et al., 2005) and on the apical pool of Hh released from Hh-producing cells (Ayers et al., 2010), we examined the role of Disp in Hh trafficking. We reasoned that in Hh-producing cells, Disp might be required for trafficking of Hh toward the apical pole of the plasma membrane. To test this, we examined the subcellular distribution of Hh in cells lacking Disp activity by conventional (permeabilized discs) or extracellular (nonpermeabilized discs) antibody staining, which reveal the total and the cell-surface Hh pools, respectively. Conventional staining showed a substantial increase in Hh levels, evenly distributed along the apico-basal axis of *disp* mutant cells and *disp* mutant discs, and no defects in the distribution of the apico-basal markers as compared to WT (Figures 4A–4B′, S4A–S4B′, and S4E–S4F′). Extracellular staining revealed that Hh was present at both apical and basal external surfaces of *disp* mutant cells, as in WT cells, but was more abundant at the apical pole of the mutant cells than in the adjacent WT cells (Figures 4C–4D′). This suggests that, in contrast to observations for other epithelia (Gallet et al., 2003), Disp is not required for the trafficking of Hh to the apical domain of the wing imaginal disc. We checked that this extracellular detection was not due to the contribution of Hh secreted from WT surrounding cells by repeating the staining on discs entirely mutant for *disp* activity. As in our clonal analysis, we detected a substantial accumulation of cell-surface Hh at the apical surface of Hh-producing cells (Figures S4C–S4D′). These data suggest that, despite the lack of Disp activity, Hh is delivered through primary secretion to the apical side of the epithelium and accumulates externally. It is likely that this accumulation leads to a traffic jam in the Hh secretory pathway, resulting in an overall accumulation of intracellular Hh. We therefore conclude that the principal role of Disp is to regulate Hh once it has reached the external side of the apical plasma membrane of producing cells.

Hh Internalization in Producing Cells Is Impaired in *disp* Mutants

How can we reconcile the apical accumulation of extracellular Hh in *disp* mutant discs and the lack of long-range Hh activity? As apical Hh is internalized and Hh gradient activity is regulated by Rab5-/Rab4-dependent mechanisms, we explored the possibility that Disp regulates the uptake of apical Hh in Hh-producing cells. We therefore expressed Hh-GFP in the posterior compartment of *disp* mutant discs and assayed for colocalization with FM4-64. The lack of *disp* activity resulted in an impairment of Hh-GFP endocytosis at all the points tested because dually labeled Hh-GFP/FM4-64 vesicles were barely observed in this background (Figures 4E–4L; Table 1). However, the distribution of internalized FM4-64 vesicles was similar in WT (Figures 2E–2I) and *disp* mutant discs (Figures 4I–4L), suggesting that the general endocytic process was not affected in the absence of Disp.

To confirm this finding, we compared the distribution of vesicles positive for FM4-64 or for Dextran, another endocytic marker, in WT and *disp* mutant cells within the same disc. We

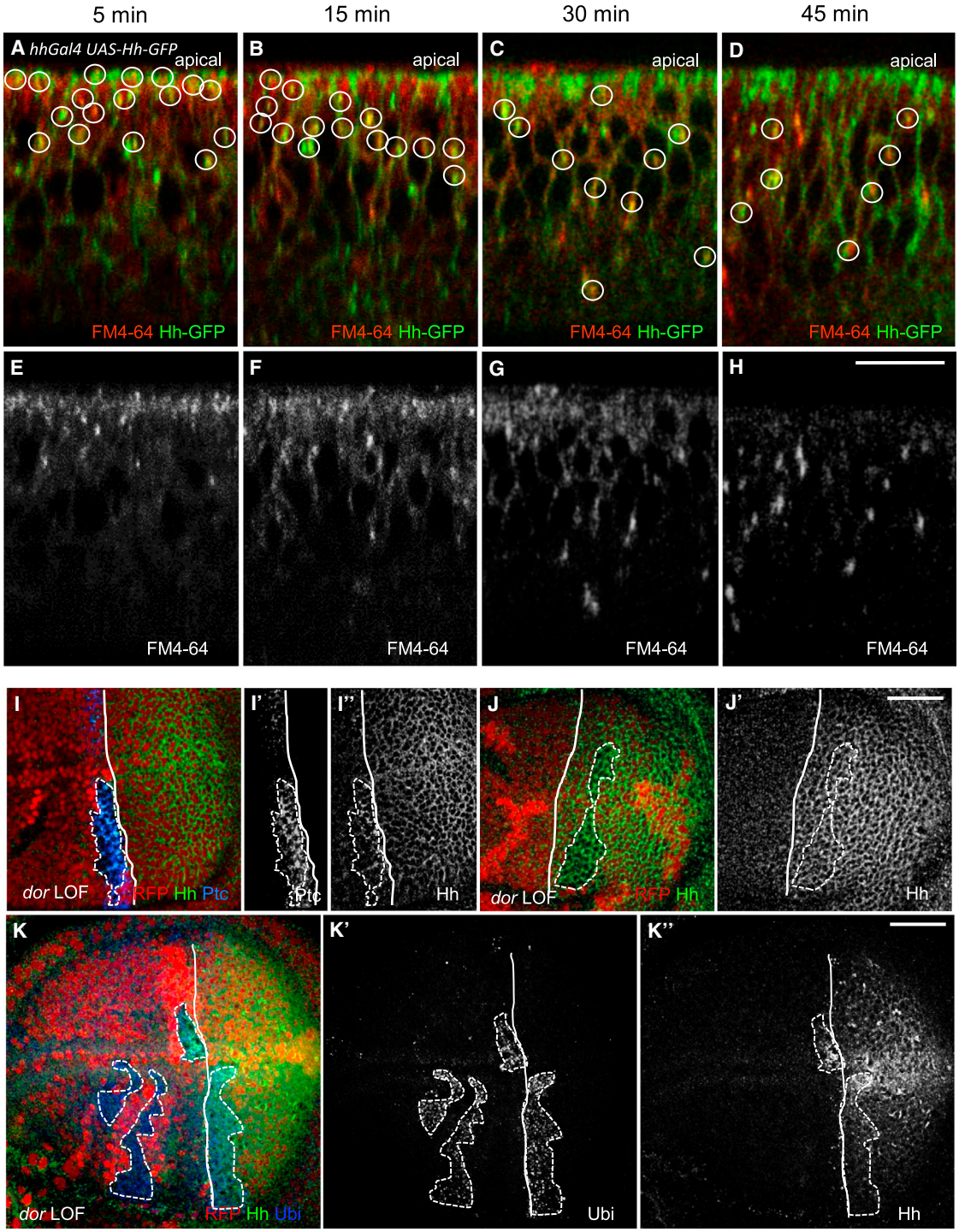

Figure 2. Endocytosis of Hh-GFP in Producing Cells Does Not Lead to Hh Degradation

(A–H) Live wing imaginal discs expressing Hh-GFP in the posterior compartment incubated with the endocytic marker FM4-64 (red) and chased for the indicated times. (A–H) Single XZ sections in the posterior compartment perpendicular to the D/V axis. (A–D) Numerous Hh-GFP-containing structures are endocytic by nature as shown by their colocalization with the endocytic marker FM4-64 (circles). (E–H) Images depict FM4-64-positive vesicles over different periods. Note that the subcellular distribution of endocytic vesicles trafficks from the apical to the basolateral surface in a time-dependent manner. Note that the lowering of Hh-GFP/FM4-64 dually labeled vesicles correlates with the trafficking of FM4-64 vesicles from the apical to the basolateral surface.

(I–L″) Hh levels are unaffected in posterior *dor* deficient cells. Wing discs with *dor* mutant clones marked by the absence of RFP and delineated by dashed white lines. Projections of four confocal views 250 nm apart passing through the lateral cell membranes, stained for Hh (green and gray; J, J″, K, K′, L, and L″), Ptc (blue and gray; J and J′), and Ubi (blue and gray; L and L′). *dor* mutant cells in the anterior compartment show an accumulation of Ptc and Hh (J–J″) and Hh and Ubi (L–L″). Quantification of Hh and Ptc staining intensity in the anterior compartment (J–J″) revealed a substantial increase in *dor*-deficient cells as compared to WT

(legend continued on next page)

Table 1. Quantification of FM4-64, Hh-GFP (in WT and disp$^{-/-}$ discs), Hh-N-GFP, or GFP-Hh-C-Positive Structures

Hh-GFP Constructs	Fluorescence Detected	Puncta # after 5 min Chase	Puncta # after 15 min Chase	Puncta # after 30 min Chase	Puncta # after 45 min Chase
Hh-GFP (WT)		(n = 11)	(n = 14)	(n = 14)	(n = 9)
	FM4-64$^+$	328	406	402	252
	GFP$^+$	403	506	512	326
	GFP$^+$FM4-64$^+$ (double positive)	231	256	210	92
	GFP$^+$FM4-64$^+$/GFP$^+$ (endosomal fraction of Hh)	57.1%	50.8%	41.1%	28.3%
Hh-GFP (*disp*$^{-/-}$)		(n = 6)	(n = 9)	(n = 9)	(n = 6)
	FM4-64$^+$	182	265	258	169
	GFP$^+$	228	351	333	217
	GFP$^+$FM4-64$^+$ (double positive)	2	5	3	1
	GFP$^+$FM4-64$^+$/GFP$^+$ (endosomal fraction of Hh)	0.9%	1.4%	0.9%	0.5%
Hh-N-GFP		–	(n = 9)	–	–
	FM4-64$^+$	ND	276	ND	ND
	GFP$^+$	ND	432	ND	ND
	GFP$^+$FM4-64$^+$ (double positive)	ND	3	ND	ND
	GFP$^+$FM4-64$^+$/GFP$^+$ (endosomal fraction of Hh-N)	ND	0.925%	ND	ND
GFP-Hh-C		–	(n = 6)	–	–
	FM4-64$^+$	ND	190	ND	ND
	GFP$^+$	ND	507	ND	ND
	GFP$^+$FM4-64$^+$ (double positive)	ND	0	ND	ND
	GFP$^+$FM4-64$^+$/GFP$^+$ (endosomal fraction of Hh-C)	ND	0	ND	ND

Total number of internalized FM4-64- or Hh-GFP-positive structures for each incubation time in posterior cells of four to five discs (FM4-64 chase starts at t = 0; n = total number of Z sections 2 μm apart). There is no statistically significant difference for the FM4-64 endocytic vesicles over time (p = 0.48 [ANOVA]). ND, not determined.

found that the distribution of FM4-64- or Dextran-positive vesicles were similar in both cell types (Figures 4M–4P′). We also found that Hh uptake and Ptc expression in *disp* mutant cells could be rescued by the expression of a functional tagged form of Disp (Disp-HA or Disp-GFP; Figures S4H–S4I′ and S5G–S5I, respectively). The distribution of Disp-HA was analyzed by optic and electron microscopy and showed that Disp was present at the plasma membrane, at various places such as apical, lateral, and basal (Figures S4J–S4P), which is compatible with a role of Disp at the plasma membrane. Thus, although Disp is dispensable for the general endocytic process, Disp activity is required for the uptake of Hh-GFP in Hh-producing cells.

Disp Is Required for the Endocytosis of Hh Provided Extracellularly

Two different mechanisms might account for the internalization of Hh in Hh-producing cells. In a one-step mechanism, the cell surface-associated Hh is directly internalized in a Disp-dependent manner. Alternatively, in a two-step mechanism, the cell surface-associated Hh is extracted into the extracellular space in a Disp-dependent manner, and is then recaptured and subsequently internalized independently of Disp. If Disp is necessary for the internalization, we reasoned that a pool of Hh secreted from WT cells (with Disp activity) and distributed at the apical surface of posterior *disp* mutant cells would not be internalized and would instead be accumulated at the cell surface.

To address these issues, we took advantage of the architecture of the wing disc, which consists of two layers of cells with apical surfaces facing each other: the columnar epithelium of the disc proper, overlayed by the squamous epithelium known as the peripodial membrane, but separated by an extracellular space (lumen). It is known that following Hh production by peripodial cells, Hh is secreted into the lumen and activates Hh-responsive targets in columnar cells (Figure 5, upper left scheme; Pallavi and Shashidhara, 2003; Vyas et al., 2008). We therefore produced Hh-GFP and Disp-HA in peripodial cells of *disp* mutant discs to provide them with Disp activity and ensure the release of Hh-GFP only from the peripodial membrane (Figure 5, upper right scheme). This strategy made it possible to monitor Hh-GFP internalization into the underlying columnar cells mutant for Disp activity, and to analyze the accumulation of extracellular Hh-GFP at their apical surface. With an extracellular staining of Hh-GFP in the WT background, we could show that Hh was

cells (Hh: 35.4 ± 1.22 and 19.55 ± 1.37, Ptc: 71.1 ± 3.9 and 31.11 ± 2.31, in *dor* mutant and WT cells, respectively). (K–L″) In the posterior compartment, no significant difference in Hh expression levels was detected between *dor* mutant and surrounding WT cells (K and K′: 36.01 ± 3.42 and 36.49 ± 3.42, respectively; p value = 0.78, t test), whereas Ubi staining increased (L′). The anterior/posterior compartment boundary is indicated by a white line. Six to 14 anterior and posterior clones were examined.

(H, J′, and K″) Scale bars represent 20 μm. See also Figure S2.

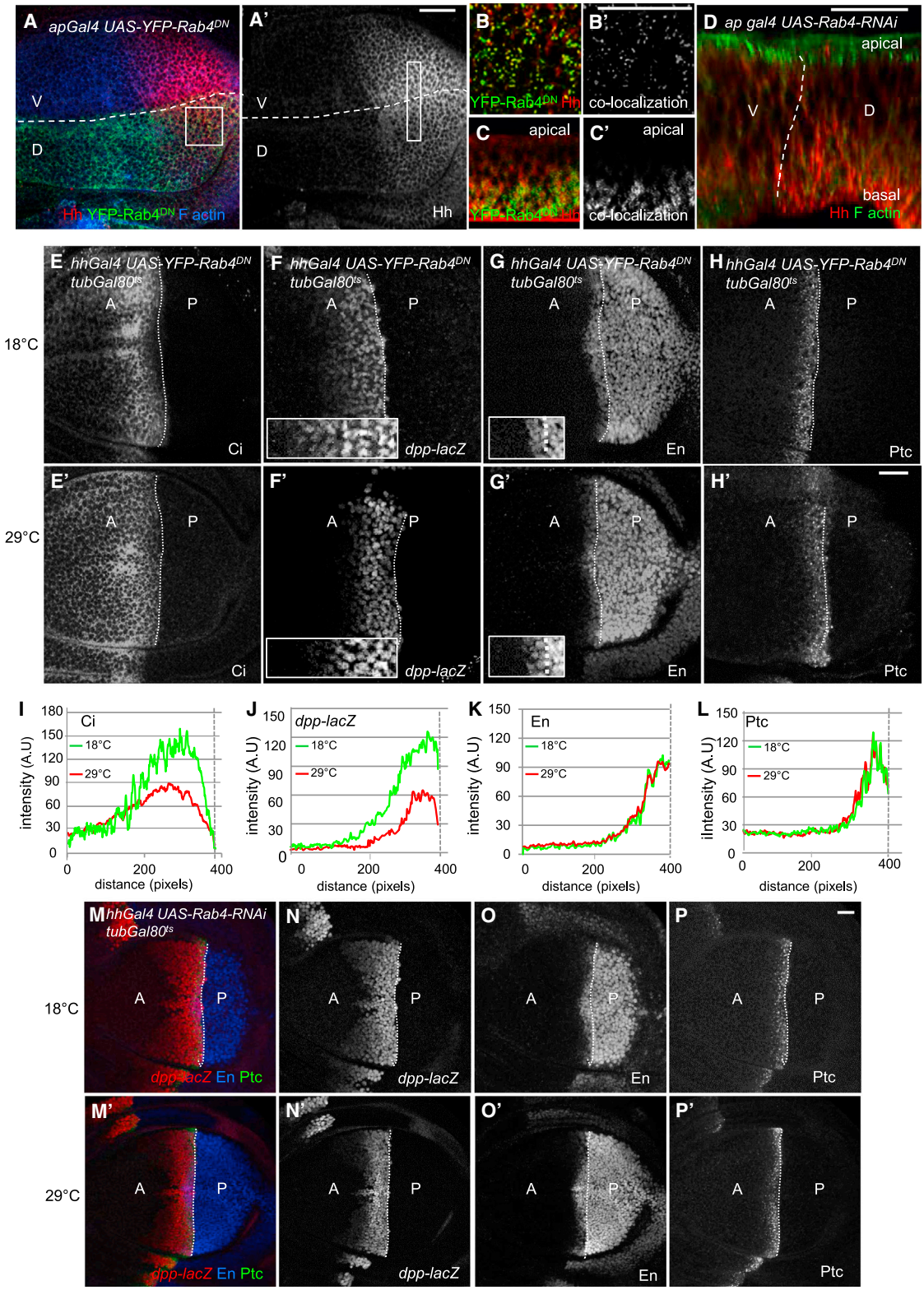

Figure 3. Rab4^{DN} Expression Alters the Subcellular Distribution of Hh and Decreases Long-Range Activity

(A–C′′) Discs after 16 hr of YFP-Rab4^{DN} or (D) Rab4-RNAi expression in the dorsal compartment stained for Hh (red), F actin (blue in A–C and green in D), and YFP-Rab4^{DN} (green in A–C). (A–A′′) Single confocal section 3 μm below the apical surface. (A′) Hh staining is shown in gray. The rectangle in A′ corresponds to the area quantified in Figure S3E. (B and B′) Magnification of the white square defined in (A) showing a merged image (B), and the colocalization of Hh and Rab4^{DN} (B′).

(legend continued on next page)

present at the outer leaflet of peripodial cells, indicating that it has been correctly secreted (data not shown). With conventional staining, luminal Hh-GFP was barely detectable in the WT background (Figures 5A–5A″). Nevertheless, we observed Hh-GFP-positive puncta particularly abundant at the level and below the apical membrane of columnar cells, presumably reflecting vesicular structures (Figures 5A′ and 5A″, green arrows). This prompted us to investigate the internalization of ectopically secreted Hh-GFP with FM4-64 in live discs. We observed Hh-GFP puncta at cell membranes and double-labeled FM4-64/Hh-GFP vesicles (Figures 5B–5C′), suggesting that a substantial subset of the Hh-GFP puncta (quantitative analysis showed that this subset corresponded to 46% of the total number) were derived from endocytosis into columnar cells. These results validate our strategy and confirm that extracellular Hh-GFP, secreted from peripodial cells, is taken up by endocytosis at the apical pole of columnar cells with functional Disp activity.

When columnar cells, but not peripodial cells, lacked *disp* activity, the discs were smaller and more closely resembled those observed when Disp was absent from both epithelia (Figures 5A and 5D). Hh-GFP particles in peripodial cells looked similar in WT and in rescued *disp* mutant cells, both expressing the Disp-HA transgene, suggesting that a similar form of Hh-GFP in both genotypes is released from peripodial cells (Figures S5A–S5D′). In contrast to what was observed in the WT background, secreted Hh-GFP accumulated within the lumen of *disp* mutant discs (Figures 5D–5D″). Uptake assays showed that, despite FM4-64 internalization (Figure 5F), no colocalization of Hh-GFP and FM4-64 was observed (Figures 5E and 5F). Hh-GFP remained at the apical membrane of columnar cells lacking Disp activity (Figures 5F and 5F′ and inset). An uncleavable form of Hh (Hh-U^{NHA}; Chu et al., 2006) expressed in peripodial or columnar cells was not secreted, confirming that the Hh-GFP detected in the luminal space corresponds indeed to the processed form of Hh and not to the full-length Hh-GFP (Figures S5E–S5F′).

Altogether, these results are consistent with the hypothesis that the endocytosis of extracellular Hh-GFP is sensitive to Disp. These data strongly suggest that Disp is required for the internalization of secreted Hh in Hh-producing cells.

DISCUSSION

Here we show that the multipass transmembrane protein Disp has a critical role in the internalization of Hh in Hh-producing cells. Furthermore, our studies reveal that both Rab5 and Rab4, respectively involved in endocytosis and recycling, were instrumental in regulating long-range Hh activity. We propose that Disp-dependent endocytosis and subsequent recycling contribute to the establishment of the Hh morphogen gradient.

The apical decrease and basolateral accumulation of cholesterol-modified Hh in Disp mutant *Drosophila* embryos led to the suggestion that Disp was necessary for the trafficking of Hh to the apical pole of producing cells (Gallet et al., 2003). We show here that, in wing imaginal discs lacking Disp function, Hh protein is present at the apical surface of Hh-producing cells. These findings suggest that in these cells, the secretion of Hh to the outer leaflet of the plasma membrane is independent of Disp activity. Results also suggest that Disp may regulate Hh secretion once Hh has accumulated at the external surface of the plasma membrane, consistent with the distribution of Disp at the plasma membrane.

Disp may facilitate the direct release of Hh from the plasma membrane into the extracellular space. Indeed, the vertebrate homolog of Disp, Dispatched-A (DispA), has recently been shown to act in synergy with the vertebrate-specific Scube2, a secreted glycoprotein, to control vertebrate Hh release (Creanga et al., 2012; Tukachinsky et al., 2012). DispA and Scube2 recognize and bind directly to different structural aspects of the cholesterol attached to vertebrate Hh and act in a sequential manner, with DispA transferring cholesterol-modified Hh to Scube2, possibly at the plasma membrane. In this model, Scube2 shields the cholesterol anchor of Hh, allowing this protein to be transported in a hydrophilic environment. There is no Scube2 homolog in *Drosophila*, raising questions about whether a similar process regulates the extraction of *Drosophila* Hh from the plasma membrane bilayer.

We provide evidence here for an additional role of Disp. We show that, after reaching the plasma membrane, cholesterol-modified Hh is endocytosed in a Disp-dependent manner (Figures 2 and 4). In contrast to the findings of a previous report suggesting a role for Disp in the regulation of general vesicular trafficking (Callejo et al., 2011), we demonstrate here that Disp does not affect the internalization of the widely used endocytic markers FM4-64 and Dextran (Figure 4). We confirmed that Disp did not regulate general vesicular trafficking because, in *disp* mutant animals, no defect was observed in the subapical localization of the E-cad transmembrane marker (this work) or in the Notch or Wingless pathways, which require tight regulation of receptor and ligand internalization for correct activation (Le Borgne et al., 2005; Seto and Bellen, 2006; data not shown).

What is the role of Hh endocytosis in Hh-producing cells? Endocytosis could be required for the degradation of an unnecessary pool of Hh and regulation of the overall level of Hh

Quantifying six confocal sections/disc on 16 discs indicates that 85% of the brightest $Rab4^{DN}$ punctae colocalized with Hh. (C and C′) Single confocal XZ section in the posterior-dorsal compartment. $Rab4^{DN}$ and Hh localize at the lateral and basolateral planes.

(D) Single confocal XZ section overlapping the dorso-ventral compartment of disc expressing Rab4-RNAi in the dorsal compartment. The white broken lines delimit the ventral (V) and dorsal (D) compartments.

(E–P′) *hhGal4 UAS-YFP-Rab4^{DN}*, *tubGal80^{ts}* (E-H′) or *hhGal4 UAS-Rab4-RNAi*, *tubGal80^{ts}* (M–P′) discs raised at 18°C ($Gal80^{ts}$ permissive temperature) up to L3 for controls or reared at 29°C ($Gal80^{ts}$ restrictive temperature) for 20 (E–H′) or 30 (M–P′) hours to allow YFP-$Rab4^{DN}$ or Rab4-RNAi expression in Hh-producing cells. Discs were stained for Ci (E and E′), β-gal (reflecting expression of the reporter gene *dpp-lacZ*; F, F′, N, and N′), En (G, G′, O, and O′), or Ptc (H, H′, P, and P′).

(I–L) Quantification of Ci, *dpp-lacZ,* En, or Ptc staining intensity at both permissive (green lines) and restrictive (red lines) temperatures, of discs stained and imaged in parallel under identical conditions. At least eight discs from each phenotype were analyzed. Quantifications are plotted as a function of distance from the A/P boundary (indicated by a dotted white or black lines in E–H′ and I–L, respectively) and are for the discs shown in E–H′, but representative of all examined discs.

(A′, B′, D, H′, P) Scale bars represent 20 μm. See also Figure S3.

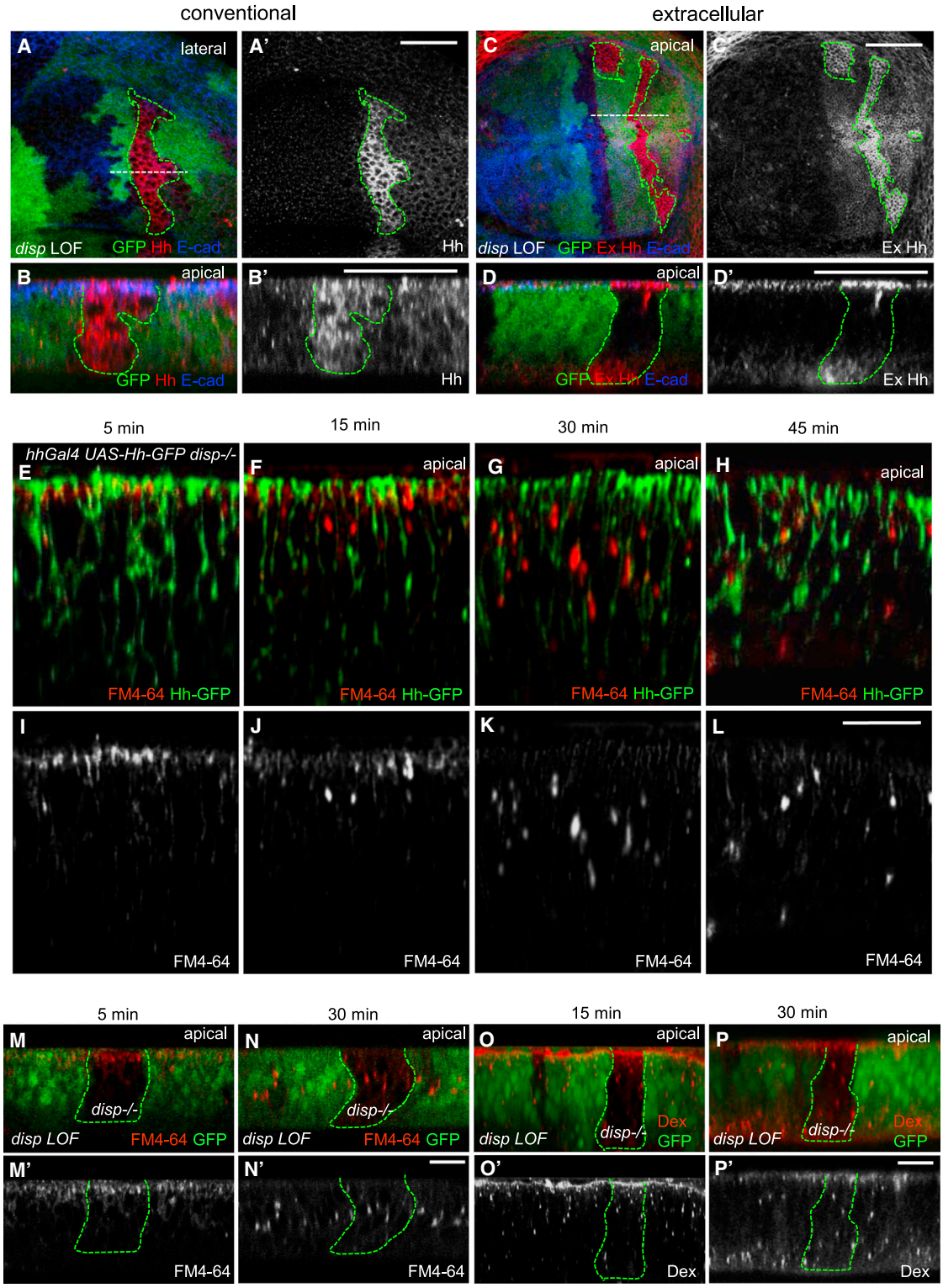

Figure 4. Disp Is Required for the Endocytosis of Hh in Producing Cells

(A–D′) Discs with *disp* mutant clones in Hh-producing cells were analyzed by conventional (A–B′) or extracellular staining for Hh (C–D′). Clones are marked by the absence of GFP and the dashed green line. White dotted lines in (A) and (C) indicate the position of the Z-sections shown in (B) and (D). (A–B′) Hh (red or gray) is strongly accumulated in *disp* mutants clones. (B–B′) The Z-section shows an even distribution of Hh along the apico-basal axis. Note that Hh also accumulates above the E-cad (blue). (C–D′) Extracellular labeling reveals the distribution of Hh at the apical surface of the epithelium. Blocking Disp activity leads to a strong accumulation of Hh at the apical pole as compared to surrounding WT cells. E-cad marks apical junctions.

(legend continued on next page)

produced by posterior cells. However, this seems unlikely because we found no evidence for Hh degradation in these cells (Figure 2). Furthermore, if endocytosis was necessary for Hh degradation, then the inhibition of Hh endocytosis would not be expected to decrease the range of Hh activity. However, the use of $Rab5^{DN}$ to inhibit Hh endocytosis in posterior cells resulted in the decrease of expression of the long-range target *dpp*, suggesting that endocytosis was required for the long-range activity of Hh (Figure S3). Following $Rab5^{DN}$ expression, the decrease in Hh target expression was weaker than that observed in *disp* mutant animals (Burke et al., 1999). There are two nonmutually exclusive reasons for this: the use of $Rab5^{DN}$ to block Hh endocytosis without affecting cell viability may not have resulted in a complete blockage of Hh internalization, and the residual levels of endocytosis may have resulted in significant long-range Hh activity. Alternatively, the *disp* phenotype may result in cumulative defects of Hh extraction from the plasma membrane and endocytosis.

The regulation of Hh internalization by Disp provides new perspectives regarding our understanding of Disp function. The enzymatic function of this protein remains unknown, but it has been assigned to the RND transporter family based on its conserved residues. The members of this family are prokaryotic proton-driven transporters providing resistance to drugs or heavy metals by exporting these substrates out of the cell. Mutations affecting the aspartic acid residues in transmembrane domain 4, essential for proton translocation across the membrane in other RND members (Goldberg et al., 1999), affect Disp activity (Ma et al., 2002). Because RND proteins are proton gradient-driven transporters, Disp might be internalized and therefore function in an acidic compartment, such as endocytic vesicles, which possess a transmembrane proton gradient. Hh and Disp have been detected in internalized vesicles (Callejo et al., 2011), suggesting that internalized Disp may be required for the homeostasis of a Hh-specific secretory compartment, such as recycling compartments. This suggests that Disp may display at least two functions: in posterior cells, in which the Hh receptor Ptc is absent, Disp may bind Hh directly, thereby promoting its internalization; whereas the enzymatic Disp activity may be required in endocytic compartments containing both proteins. It is possible that Disp functions in this endocytic compartment by associating Hh with dedicated proteins serving as carriers for its long-range transport. Interestingly, the long-range activity of Hh depends on the clustering of Hh oligomers with heparan sulfate proteoglycans and packaging into lipoprotein particles (Panáková et al., 2005; Vyas et al., 2008). Thus, endocytic and vesicular Disp activity may be required for the formation of an active pool of Hh, in preparation for its extracellular transportation.

We previously provided genetic evidence showing that the spread of the apical pool of Hh causes the long-range induction of low-threshold targets (Ayers et al., 2010). The data presented here suggest that Hh is recycled to the apical membrane after endocytosis (Figure 6). Indeed, the expression of a $Rab4^{DN}$ variant, which has been shown to impair recycling from early endosomes to the plasma membrane in mammalian cells (de Renzis et al., 2002), induced the basal relocalization of Hh and a decrease in the expression of long-range targets (Figure 3). These data suggest that the apical recycling is probably required for the long-range activity of Hh. Alternatively, it has been suggested that Hh endocytosis is required for the transcytosis of Hh from the apical to the basal poles of producing cells (Callejo et al., 2011), which correspond to a distance of about 40 μm in these cells. However, we found no evidence for transcytosis in this study. We think that the development of new tools for tracking single molecules will be required for investigations of the trafficking of internalized Hh in producing cells.

What can be the form of the re-launched Hh protein and why should endocytosis be required for this? We and others suggested that Hh and Hh-related peptides can be secreted on exovesicles (Tanaka et al., 2005; Liégeois et al., 2006; Gradilla et al., 2014; Matusek et al., 2014). Exovesicles may be generated by plasma membrane budding or by fusion of endocytic multivesicular bodies with the plasma membrane, leading to the release of multivesicular body intraluminal vesicles into the extracellular space (Colombo et al., 2014). Our data suggest that defects in multivesicular body trafficking in Hh-producing cells do not correlate with defects in Hh signaling (Matusek et al., 2014). Interestingly, Rab4 is present in exovesicles from human reticulocytes (Vidal and Stahl, 1993) and colocalizes in vivo with Wingless in secreted particles (Gross et al., 2012). It is thus possible that endocytosis is necessary for Hh to traffic through a Rab4 recycling compartment before being targeted to a plasma membrane subdomain, where Hh would be prepared to be loaded on exovesicles.

In summary, we show that the mechanism of Hh release is not based purely on the primary secretion of Hh. Our results reveal the existence of a Disp-dependent secondary secretion mechanism for Hh, involving the internalization and recycling of this protein before its release and long-range transport.

EXPERIMENTAL PROCEDURES

Drosophila Stocks and Clonal Analysis

The following stocks were used in this study: w^{1118}, *ap-Gal4*, *hh-Gal4*, *ubx-Gal4*, *tub-Gal80^{ts}*, *YFP-UAS-Rab5^{CA}*, *YFP-UAS-Rab4^{DN}* (Zhang et al., 2007), and were obtained from the Bloomington Stock Center. The UAS-RNAi line against Rab4 $Rab4^{24672GD}$) was from Vienna *Drosophila* RNAi Center. *UAS-Dicer2* (Bloomington), *UAS-Hh-GFP* (Torroja et al., 2004), *UAS-Disp^{HA}* (Burke et al., 1999). *disp^{SO37707}* is a null allele (Burke et al., 1999); *dor^{8}FRT19A/FM7actGFP* was from S. Mayor; the nuclear *dpp-nuc-lacZ^{P10638}* reporter was from X. Lin. The Rab5::EGFP knockin line (Fabrowski et al., 2013) was from De Renzis. Overexpression clones in the wing imaginal discs were

(E–L) Live wing imaginal discs expressing UAS-Hh-GFP in the posterior compartment of *disp* mutant discs incubated with the endocytic marker FM4-64 (red) and chased for the indicated times. Single XZ sections in the posterior compartment perpendicular to the D/V axis. (E–H) Almost no vesicles double-stained for Hh-GFP and FM4-64 are observed. (I–L) Images depict the up-taken FM4-64 vesicles over the indicated periods. Three to five discs were examined for each incubation time.

(M–P′) In discs with *disp* mutant clones the distribution of FM4-64 (M–N′) or Dextran-Texas red (Dex, O–P′) positive particles were similar in *disp* mutant cells and the surrounding WT cells. Mutant clones are labeled by the absence of GFP and by a dotted green line.

(A′, B′, C′, D′, L, N′, and P′) Scale bars represent 20 μm. See also Figure S4.

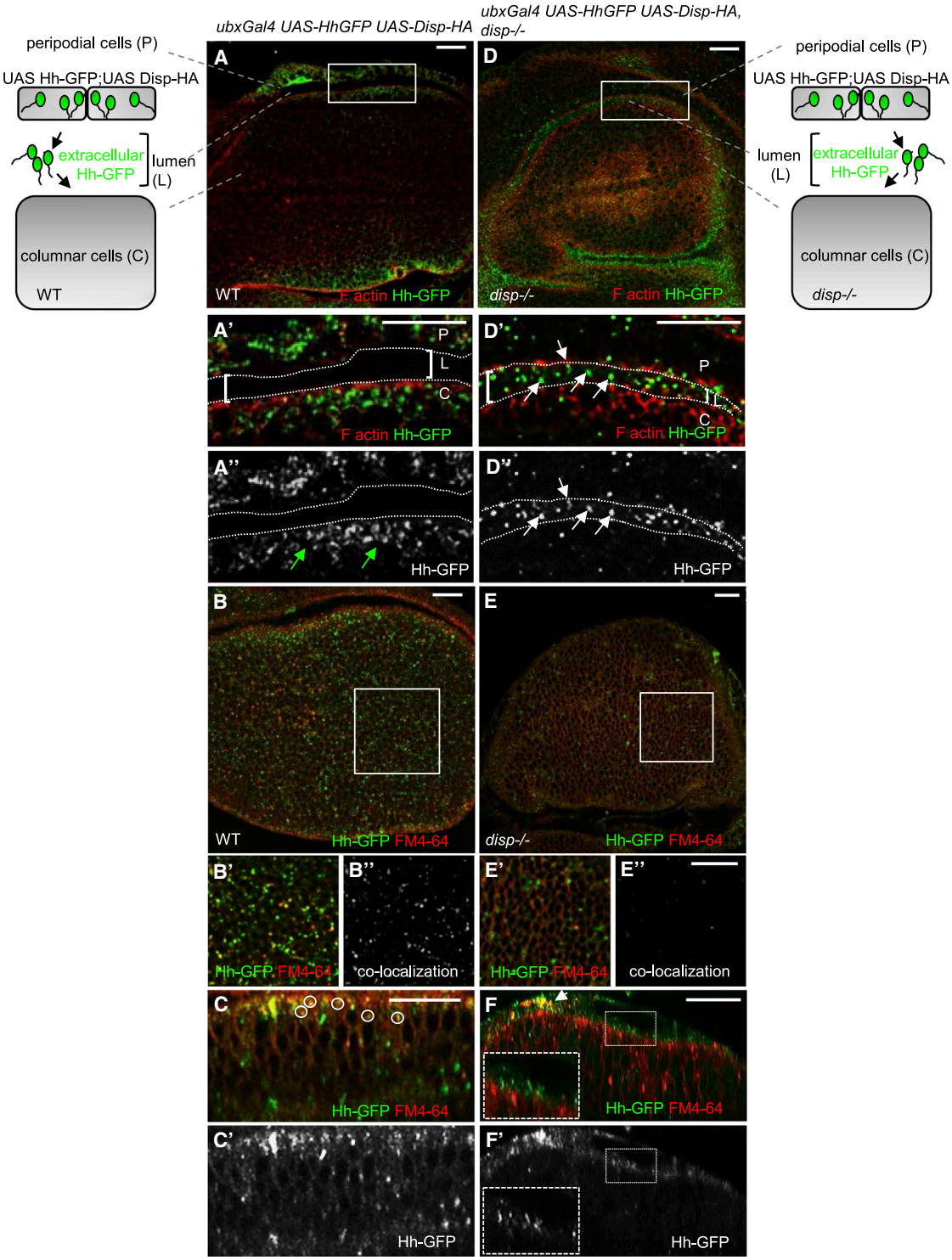

Figure 5. The Endocytosis of Secreted Hh Is Disp Dependent

(A–F′) Disc overexpressing Hh-GFP and Disp-HA in peripodial cells in the WT (A–C′) and *disp* mutant (D–F′) backgrounds. (A–A′′) Conventional staining for Hh-GFP (green, gray). Projections of four confocal sections 250 nm apart at the apical surface. (A′ and A′′) High-magnification images of the inset demarcated by a rectangle in (A). Hh-GFP is present in both peripodial and columnar cells. Note the presence of Hh-GFP puncta at the apical pole of cells facing the lumen (green arrows in A′′). The lumen between the two epithelia is delimited by brackets and a dotted line in A′. (B–C′) Images show single confocal section of live discs incubated for 15 min with the endocytic marker FM4-64. (B′–B′′) Magnification of the boxed area in (B) in columnar cells. Overall, 46% of all Hh-GFP puncta colocalize with FM4-64. (C and C′) Single XZ confocal section. The dually labeled vesicles are circled. (D–D′′) Projections of four confocal sections 250 nm apart at the apical surface. The *disp* mutant discs are smaller than the WT discs. (D′–D′′) High-magnification images of the boxed area in (D) showing a strong

(legend continued on next page)

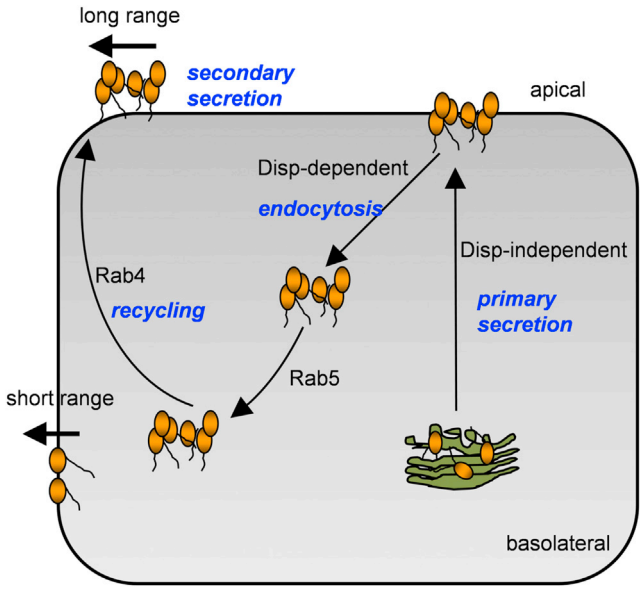

Figure 6. A Model for Hh Trafficking in Hh-Producing Cells

The intracellular pool of Hh (orange particles) is targeted to the apical plasma membrane in a Disp-independent manner. Once at the outer leaflet of the plasma membrane, Disp contributes to the apical endocytosis of Hh in posterior cells. Hh is internalized in Rab5 early endosomes, subsequently following the canonical rapid recycling pathway regulated by Rab4. The absence of Disp, Rab5, or Rab4 activity decreases the long-range activity of Hh.

obtained with the "flip-out" technique (Basler and Struhl, 1994), using the *actin>CD2>Gal4* transgene recombined with the *UAS-GFP* transgene to mark the clones or the *abx>lacZ>Gal4* transgene. Clones were induced by heat shocking L1 larvae at 37°C for 10 min. The larvae were then allowed to grow at 25°C until L3 stage, except for *UAS-YFP-Rab5^{CA}* experiments that were kept at 18°C. Transient expression of the *UAS* constructs using the *Gal4; tub-Gal80^{ts}* system was accomplished by keeping the fly crosses at 18°C and inactivating the Gal80^{ts} for 16–24 hr at restrictive temperature (29°C). Recombinant chromosomes were created for *hh-Gal4, disp^{SO37707}*; *ubx-Gal4, disp^{SO37707}*; *UAS-Disp^{HA}*, *disp^{SO37707}*, by classical genetic techniques. Rescue experiments were carried out by crossing *y,w,hs-flp; dpp-LacZ; hh-Gal4, disp^{SO37707} FRT82B/TM6b to w; UAS-Disp^{HA}; disp^{SO37707} FRT82B /TM6c.*

Mutant clones for *disp and dor^{8}* were obtained by FRT-FLP-mediated recombination (Xu and Rubin, 1993). Clones were induced by heat shocking L1 larvae for 30 min and then allowing the larvae to grow at 25°C. The genotypes of the flies for clone induction were *yw hs-flp 122; dpp-LacZ; disp^{SO37707} FRT82B/ubiGFP FRT82B* and *dor^{8}FRT19A/ubiRFP FRT19A hs-flp122.*

Imaginal Disc Immunostaining, Image Capture, and Analyses

Immunostaining was performed as previously described (Gallet et al., 2006). Antibodies were used at the following dilutions: mouse 4D9 monoclonal anti-En (Development Studies Hybridoma Bank University of Iowa – DSHB), 1/1,000; rabbit polyclonal anti-En (Santa Cruz), 1/1,000; mouse monoclonal anti-Ptc 1/400 (Strutt et al., 2001); rat 2A1 monoclonal anti-Ci antibody, 1:20 (DSHB); chicken polyclonal anti-βgal, 1/1,000 (Gen Tex); affinity-purified rabbit "Calvados" polyclonal anti-Hh, 1:400 (Gallet et al., 2003); rabbit polyclonal anti-Rab5 (Abcam), 1:100; rat DCAD2 polyclonal anti-DE-cadherin (DSHB), 1/50; rabbit polyclonal anti-GFP (Biolabs), 1/400; mouse monoclonal anti-GFP (Roche), 1/200; rat polyclonal anti-HA (Roche) 1/50; mouse anti-Ubi (clone FK2; ENZO, Life-Science) 1/1,000. Fluorescent secondary antibodies were used at 1/100 for Cy3-conjugated donkey anti-rat, Cy3- or Cy5-conjugated goat anti-mouse, Cy3- or Cy5-conjugated goat anti-rabbit, and Cy3-conjugated donkey anti-chicken (Jackson Laboratory), and 1/500 for Alexa Fluor 488 goat anti-mouse, anti-rat, and anti-rabbit (Life Technologies). Rhodamine-phalloidin (Molecular Probes) and FluoProbes 647H–Phalloidin (Interchim) were diluted 1:200. For extracellular Hh staining, L3 larvae dissected in ice-cold PBS were fixed in PBS-2% paraformaldehyde for 15 min at room temperature and incubated in PBS-2% BSA with rabbit anti-Hh (1/400) overnight at 4°C. The cell surface staining of Hh was revealed in nonpermeabilized discs. Fluorescence images were obtained with a Leica TCS SP5 confocal microscope and processed using Adobe Photoshop 7.0. Most images are stack projections of four to eight views with 250 nm steps, or single sections at the appropriate level (apical, subapical, or lateral). *Z* sections are single sections captured as indicated on the images. Plot analyses were carried out using ImageJ software and statistical analyses with Microsoft Excel software.

Endocytosis Assays

Live discs were incubated in ice-cold Schneider's S2 medium supplemented with 10% serum and 10 μM FM4-64 FX (Invitrogen) or 0.5 mM Dextran-Texas red (Life Technologies) for 12 min at 22°C and rapidly washed. The discs were then incubated for various times for chase (up to 45 min) prior to fixation in 4% PBS.

Quantification and Statistics

Quantification of intracellular FM4-64-, Hh-GFP-, Hh-N-GFP-, or GFP-Hh-C-positive structures was performed manually. The positive structures were counted in all cells of the posterior compartment from independent and single XZ sections.

SUPPLEMENTAL INFORMATION

Supplemental Information includes Supplemental Experimental Procedures and five figures and can be found with this article online at http://dx.doi.org/10.1016/j.devcel.2014.12.004.

AUTHOR CONTRIBUTIONS

G.D. and P.P.T. conceived the experiments and wrote the manuscript. T.M. conducted the experiments on Figures 1A and 1B, 2K, 3M–3P, S2P–S2Q′, and S4J–S4L. S.P. performed the immunoelectron microscopy. G.D. conducted all other experiments.

ACKNOWLEDGMENTS

We thank M. Fürthauer and M. Labouesse for helpful comments and critical discussions on the manuscript. We also thank S. Eaton for providing the GFP-Hh-C fly line, I. Guerrero for Hh-GFP lines, and S. De Renzis for Rab5::EGFP knockin. We thank L. Lavenant-Staccini for technical assistance and Sophie Pagnotta from the Centre Commun de Microscopie Appliquée, Université de Nice Sophia Antipolis, Microscopy and Imaging Platform Côte d'Azur, MICA for technical support. This work was supported by the French

accumulation of Hh-GFP puncta within the lumen (white arrows in D′ and D′′). (D′′) The luminal space is delimited by brackets and by a dotted line. (E–F′) Single confocal sections showing uptake experiments with the endocytic marker FM4-64. Hh-GFP is not taken up by endocytosis in the absence of Disp activity and remains at the apical surface of columnar cells (magnification of the inset in F′). Note that FM4-64 is internalized in *disp* mutant columnar cells. The double staining observed at the upper left corner in (F) corresponds to a cluster of peripodial cells (arrow). Schematic representations of the experiments shown in the upper right and left columns.

(A′ and D′) P, peripodial; L, lumen; C, columnar cells.

(A, A′, B–D, D′, E, E′′, and F) Scale bars represent 20 μm. See also Figure S5.

Government (National Research Agency, ANR) through the Investments for the Future LABEX SIGNALIFE: program reference no. ANR-11-LABX-0028-01 and by the Fondation pour la Recherche Médicale: DEQ201110421324. T.M was supported by the Fondation ARC pour la Recherche Contre le Cancer.

Received: January 9, 2014
Revised: September 22, 2014
Accepted: December 1, 2014
Published: January 22, 2015

REFERENCES

Ayers, K.L., Gallet, A., Staccini-Lavenant, L., and Thérond, P.P. (2010). The long-range activity of Hedgehog is regulated in the apical extracellular space by the glypican Dally and the hydrolase Notum. Dev. Cell *18*, 605–620.

Basler, K., and Struhl, G. (1994). Compartment boundaries and the control of Drosophila limb pattern by hedgehog protein. Nature *368*, 208–214.

Bischoff, M., Gradilla, A.-C., Seijo, I., Andrés, G., Rodríguez-Navas, C., González-Méndez, L., and Guerrero, I. (2013). Cytonemes are required for the establishment of a normal Hedgehog morphogen gradient in Drosophila epithelia. Nat. Cell Biol. *15*, 1269–1281.

Briscoe, J., and Thérond, P.P. (2013). The mechanisms of Hedgehog signalling and its roles in development and disease. Nat. Rev. Mol. Cell Biol. *14*, 416–429.

Buglino, J.A., and Resh, M.D. (2008). Hhat is a palmitoylacyltransferase with specificity for N-palmitoylation of Sonic Hedgehog. J. Biol. Chem. *283*, 22076–22088.

Burke, R., Nellen, D., Bellotto, M., Hafen, E., Senti, K.A., Dickson, B.J., and Basler, K. (1999). Dispatched, a novel sterol-sensing domain protein dedicated to the release of cholesterol-modified hedgehog from signaling cells. Cell *99*, 803–815.

Callejo, A., Bilioni, A., Mollica, E., Gorfinkiel, N., Andrés, G., Ibáñez, C., Torroja, C., Doglio, L., Sierra, J., and Guerrero, I. (2011). Dispatched mediates Hedgehog basolateral release to form the long-range morphogenetic gradient in the Drosophila wing disk epithelium. Proc. Natl. Acad. Sci. USA *108*, 12591–12598.

Caspary, T., García-García, M.J., Huangfu, D., Eggenschwiler, J.T., Wyler, M.R., Rakeman, A.S., Alcorn, H.L., and Anderson, K.V. (2002). Mouse Dispatched homolog1 is required for long-range, but not juxtacrine, Hh signaling. Curr. Biol. *12*, 1628–1632.

Chu, T., Chiu, M., Zhang, E., and Kunes, S. (2006). A C-terminal motif targets Hedgehog to axons, coordinating assembly of the Drosophila eye and brain. Dev. Cell *10*, 635–646.

Colombo, M., Raposo, G., and Théry, C. (2014). Biogenesis, secretion, and intercellular interactions of exosomes and other extracellular vesicles. Annu. Rev. Cell Dev. Biol. *30*, 255–289.

Creanga, A., Glenn, T.D., Mann, R.K., Saunders, A.M., Talbot, W.S., and Beachy, P.A. (2012). Scube/You activity mediates release of dually lipid-modified Hedgehog signal in soluble form. Genes Dev. *26*, 1312–1325.

de Renzis, S., Sönnichsen, B., and Zerial, M. (2002). Divalent Rab effectors regulate the sub-compartmental organization and sorting of early endosomes. Nat. Cell Biol. *4*, 124–133.

Fabrowski, P., Necakov, A.S., Mumbauer, S., Loeser, E., Reversi, A., Streichan, S., Briggs, J.A.G., and De Renzis, S. (2013). Tubular endocytosis drives remodelling of the apical surface during epithelial morphogenesis in Drosophila. Nat. Commun. *4*, 2244.

Gallet, A., and Therond, P.P. (2005). Temporal modulation of the Hedgehog morphogen gradient by a patched-dependent targeting to lysosomal compartment. Dev. Biol. *277*, 51–62.

Gallet, A., Rodriguez, R., Ruel, L., and Therond, P.P. (2003). Cholesterol modification of hedgehog is required for trafficking and movement, revealing an asymmetric cellular response to hedgehog. Dev. Cell *4*, 191–204.

Gallet, A., Ruel, L., Staccini-Lavenant, L., and Thérond, P.P. (2006). Cholesterol modification is necessary for controlled planar long-range activity of Hedgehog in Drosophila epithelia. Development *133*, 407–418.

Goldberg, M., Pribyl, T., Juhnke, S., and Nies, D.H. (1999). Energetics and topology of CzcA, a cation/proton antiporter of the resistance-nodulation-cell division protein family. J. Biol. Chem. *274*, 26065–26070.

Gorfinkiel, N., Sierra, J., Callejo, A., Ibañez, C., and Guerrero, I. (2005). The Drosophila ortholog of the human Wnt inhibitor factor shifted controls the diffusion of lipid-modified Hedgehog. Dev. Cell *8*, 241–253.

Gradilla, A.-C., González, E., Seijo, I., Andrés, G., Bischoff, M., González-Mendez, L., Sánchez, V., Callejo, A., Ibáñez, C., Guerra, M., et al. (2014). Exosomes as Hedgehog carriers in cytoneme-mediated transport and secretion. Nat. Commun *5*, 5649.

Gross, J.C., Chaudhary, V., Bartscherer, K., and Boutros, M. (2012). Active Wnt proteins are secreted on exosomes. Nat. Cell Biol *14*, 1036–1045.

Kawakami, T., Kawcak, T., Li, Y.-J., Zhang, W., Hu, Y., and Chuang, P.-T. (2002). Mouse dispatched mutants fail to distribute hedgehog proteins and are defective in hedgehog signaling. Development *129*, 5753–5765.

Kuwabara, P.E., and Labouesse, M. (2002). The sterol-sensing domain: multiple families, a unique role? Trends Genet. *18*, 193–201.

Le Borgne, R., Bardin, A., and Schweisguth, F. (2005). The roles of receptor and ligand endocytosis in regulating Notch signaling. Development *132*, 1751–1762.

Liégeois, S., Benedetto, A., Garnier, J.M., Schwab, Y., and Labouesse, M. (2006). The V0-ATPase mediates apical secretion of exosomes containing Hedgehog-related proteins in Caenorhabditis elegans. J. Cell Biol. *173*, 949–961.

Ma, Y., Erkner, A., Gong, R., Yao, S., Taipale, J., Basler, K., and Beachy, P.A. (2002). Hedgehog-mediated patterning of the mammalian embryo requires transporter-like function of dispatched. Cell *111*, 63–75.

Mann, R.K., and Beachy, P.A. (2004). Novel lipid modifications of secreted protein signals. Annu. Rev. Biochem. *73*, 891–923.

Matusek, T., Wendler, F., Poles, S., Pizette, S., D'Angelo, G., Furthauer, M., and Therond, P.P. (2014). The ESCRT machinery regulates the secretion and long-range activity of Hedgehog. Nature *516*, 99–103.

Nakano, Y., Kim, H.R., Kawakami, A., Roy, S., Schier, A.F., and Ingham, P.W. (2004). Inactivation of dispatched 1 by the chameleon mutation disrupts Hedgehog signalling in the zebrafish embryo. Dev. Biol. *269*, 381–392.

Pallavi, S.K., and Shashidhara, L.S. (2003). Egfr/Ras pathway mediates interactions between peripodial and disc proper cells in Drosophila wing discs. Development *130*, 4931–4941.

Panáková, D., Sprong, H., Marois, E., Thiele, C., and Eaton, S. (2005). Lipoprotein particles are required for Hedgehog and Wingless signalling. Nature *435*, 58–65.

Pepinsky, R.B., Zeng, C., Wen, D., Rayhorn, P., Baker, D.P., Williams, K.P., Bixler, S.A., Ambrose, C.M., Garber, E.A., Miatkowski, K., et al. (1998). Identification of a palmitic acid-modified form of human Sonic hedgehog. J. Biol. Chem. *273*, 14037–14045.

Roessler, E., Ma, Y., Ouspenskaia, M.V., Lacbawan, F., Bendavid, C., Dubourg, C., Beachy, P.A., and Muenke, M. (2009). Truncating loss-of-function mutations of DISP1 contribute to holoprosencephaly-like microform features in humans. Hum. Genet. *125*, 393–400.

Rogers, K.W., and Schier, A.F. (2011). Morphogen gradients: from generation to interpretation. Annu. Rev. Cell Dev. Biol. *27*, 377–407.

Seto, E.S., and Bellen, H.J. (2006). Internalization is required for proper Wingless signaling in Drosophila melanogaster. J. Cell Biol. *173*, 95–106.

Sevrioukov, E.A., He, J.P., Moghrabi, N., Sunio, A., and Krämer, H. (1999). A role for the deep orange and carnation eye color genes in lysosomal delivery in Drosophila. Mol. Cell *4*, 479–486.

Strutt, H., Thomas, C., Nakano, Y., Stark, D., Neave, B., Taylor, A.M., and Ingham, P.W. (2001). Mutations in the sterol-sensing domain of Patched suggest a role for vesicular trafficking in smoothened regulation. Curr. Biol *11*, 608–613.

Tanaka, Y., Okada, Y., and Hirokawa, N. (2005). FGF-induced vesicular release of Sonic hedgehog and retinoic acid in leftward nodal flow is critical for left-right determination. Nature *435*, 172–177.

Taylor, F.R., Wen, D., Garber, E.A., Carmillo, A.N., Baker, D.P., Arduini, R.M., Williams, K.P., Weinreb, P.H., Rayhorn, P., Hronowski, X., et al. (2001). Enhanced potency of human Sonic hedgehog by hydrophobic modification. Biochemistry *40*, 4359–4371.

Tian, H., Jeong, J., Harfe, B.D., Tabin, C.J., and McMahon, A.P. (2005). Mouse Disp1 is required in sonic hedgehog-expressing cells for paracrine activity of the cholesterol-modified ligand. Development *132*, 133–142.

Torroja, C., Gorfinkiel, N., and Guerrero, I. (2004). Patched controls the Hedgehog gradient by endocytosis in a dynamin-dependent manner, but this internalization does not play a major role in signal transduction. Development *131*, 2395–2408.

Tukachinsky, H., Kuzmickas, R.P., Jao, C.Y., Liu, J., and Salic, A. (2012). Dispatched and scube mediate the efficient secretion of the cholesterol-modified hedgehog ligand. Cell Reports *2*, 308–320.

Vida, T.A., and Emr, S.D. (1995). A new vital stain for visualizing vacuolar membrane dynamics and endocytosis in yeast. J. Cell Biol. *128*, 779–792.

Vidal, M.J., and Stahl, P.D. (1993). The small GTP-binding proteins Rab4 and ARF are associated with released exosomes during reticulocyte maturation. Eur. J. Cell Biol. *60*, 261–267.

Vyas, N., Goswami, D., Manonmani, A., Sharma, P., Ranganath, H.A., VijayRaghavan, K., Shashidhara, L.S., Sowdhamini, R., and Mayor, S. (2008). Nanoscale organization of hedgehog is essential for long-range signaling. Cell *133*, 1214–1227.

Vyas, N., Walvekar, A., Tate, D., Lakshmanan, V., Bansal, D., Lo Cicer, A., Raposo, G., Palakodeti, D., and Dhawan, J. (2014). Vertebrate Hedgehog is secreted on two types of extracellular vesicles with different signaling properties. Nat. Commun *7*, 7357.

Wandinger-Ness, A., and Zerial, M. (2014). Rab proteins and compartmentalization of the endosomal system. Cold Spring Harb. Perspect. Biol. *6*, a022616.

Xu, T., and Rubin, G.M. (1993). Analysis of genetic mosaics in developing and adult Drosophila tissues. Development *117*, 1223–1237.

Zeng, X., Goetz, J.A., Suber, L.M., Scott, W.J., Jr., Schreiner, C.M., and Robbins, D.J. (2001). A freely diffusible form of Sonic hedgehog mediates long-range signalling. Nature *411*, 716–720.

Zhang, J., Schulze, K.L., Hiesinger, P.R., Suyama, K., Wang, S., Fish, M., Acar, M., Hoskins, R.A., Bellen, H.J., and Scott, M.P. (2007). Thirty-one flavors of Drosophila rab proteins. Genetics *176*, 1307–1322.

Developmental Cell

Supplemental Information

Endocytosis of Hedgehog through Dispatched Regulates Long-Range Signaling

Gisela D'Angelo, Tamás Matusek, S. Pizette, and Pascal P. Thérond

SUPPLEMENTAL DATA

Endocytosis of Hedgehog Through Dispatched Regulates Long-Range Signaling

Gisela D'Angelo[1], Tamàs Matusek, Sandrine Pizette and Pascal P. Thérond[1]

D'Angelo, Figure S1 related to Figure 1

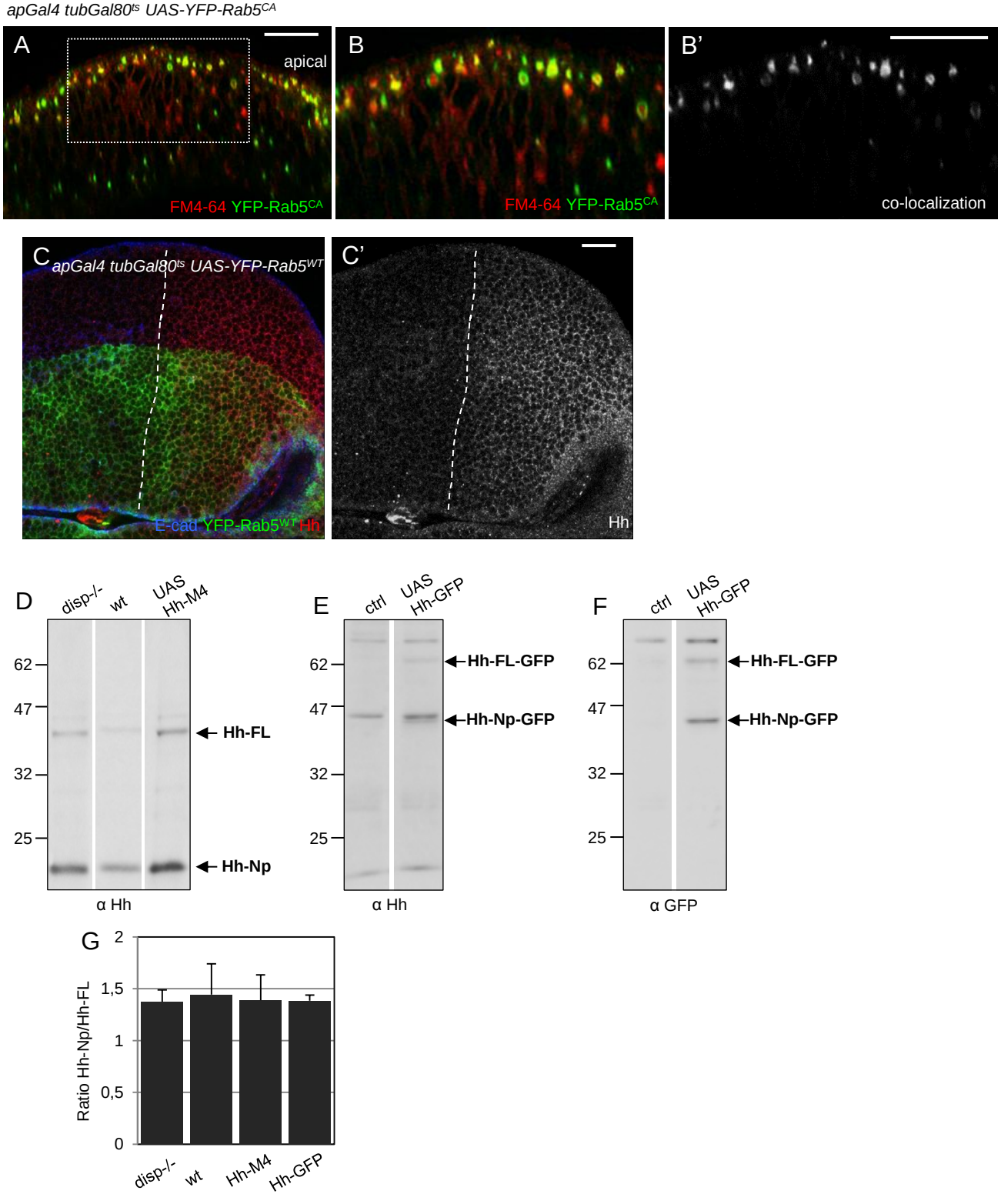

D'Angelo, Figure S2 related to Figure 2

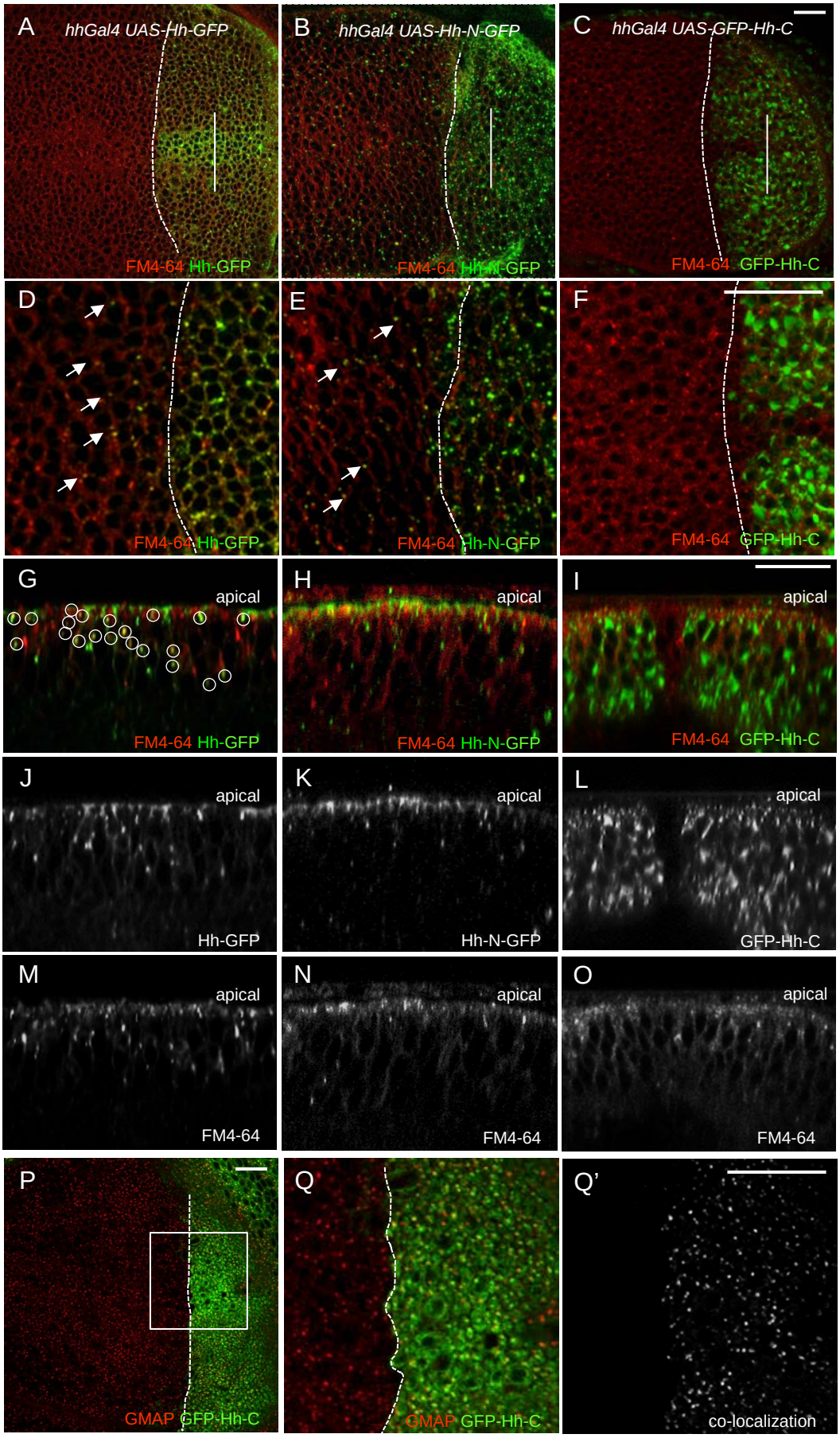

D'Angelo, Figure S3 related to Figure 3

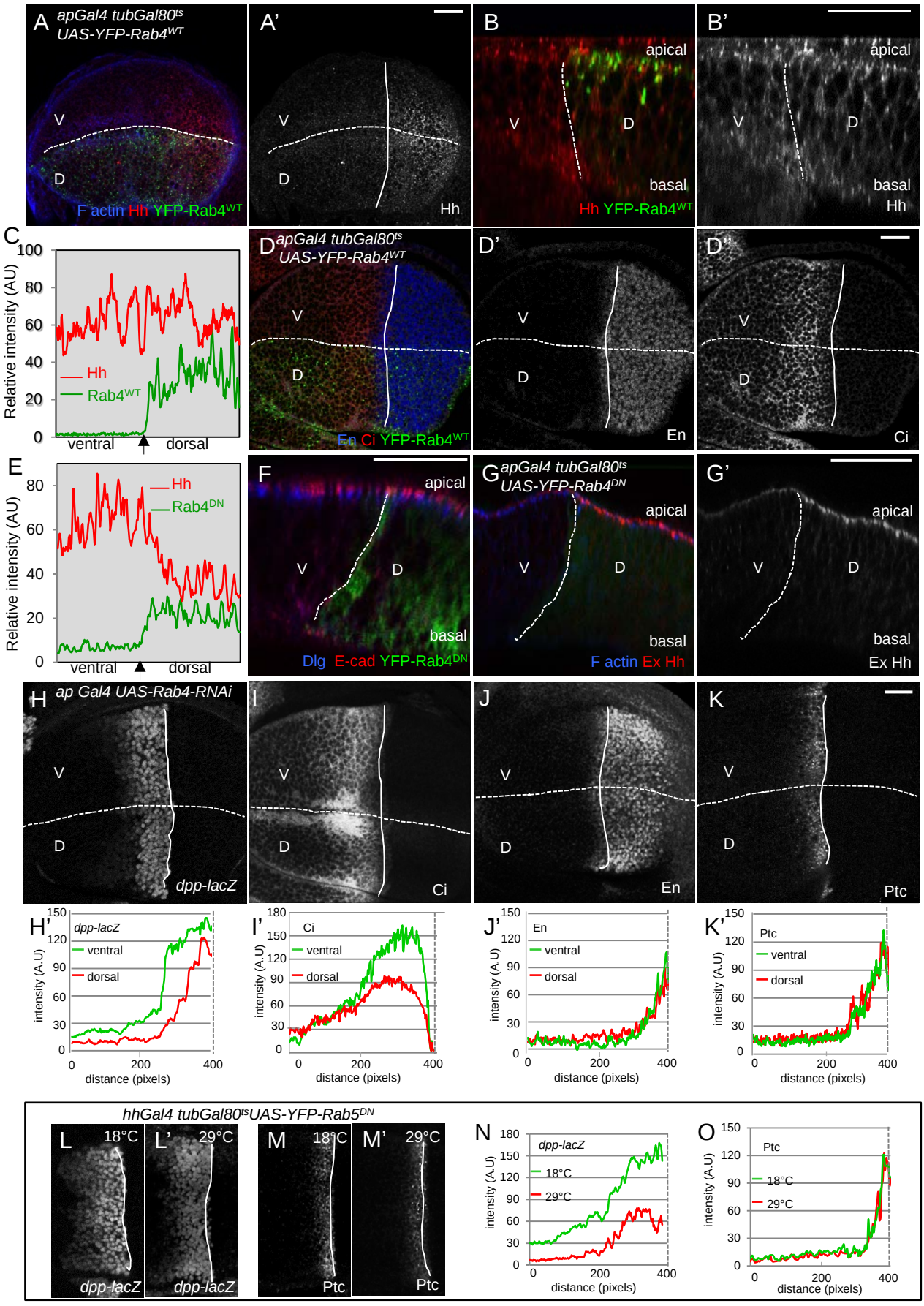

D'Angelo, Figure S4 related to Figure 4

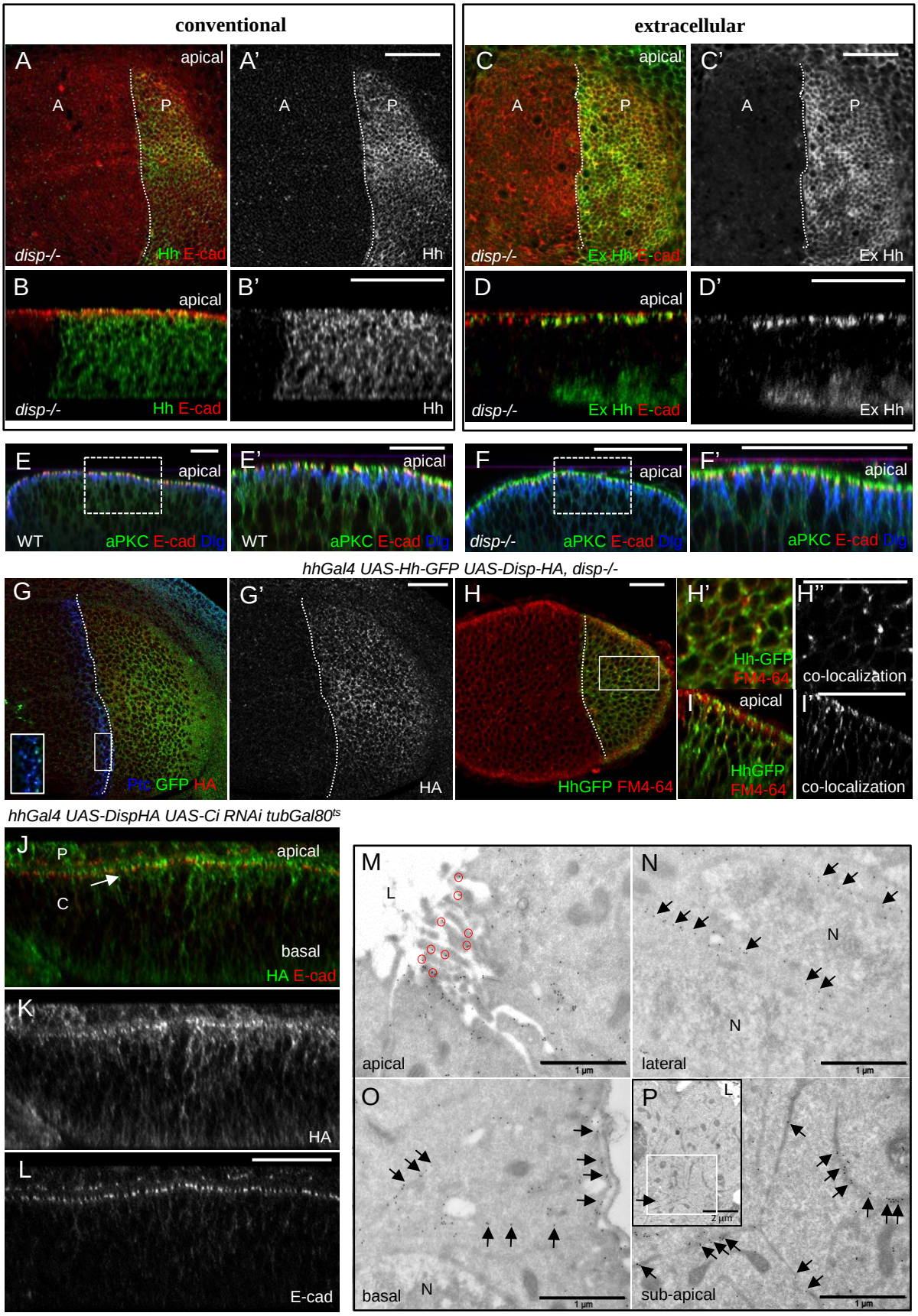

D'Angelo, Figure S5 related to Figure 5

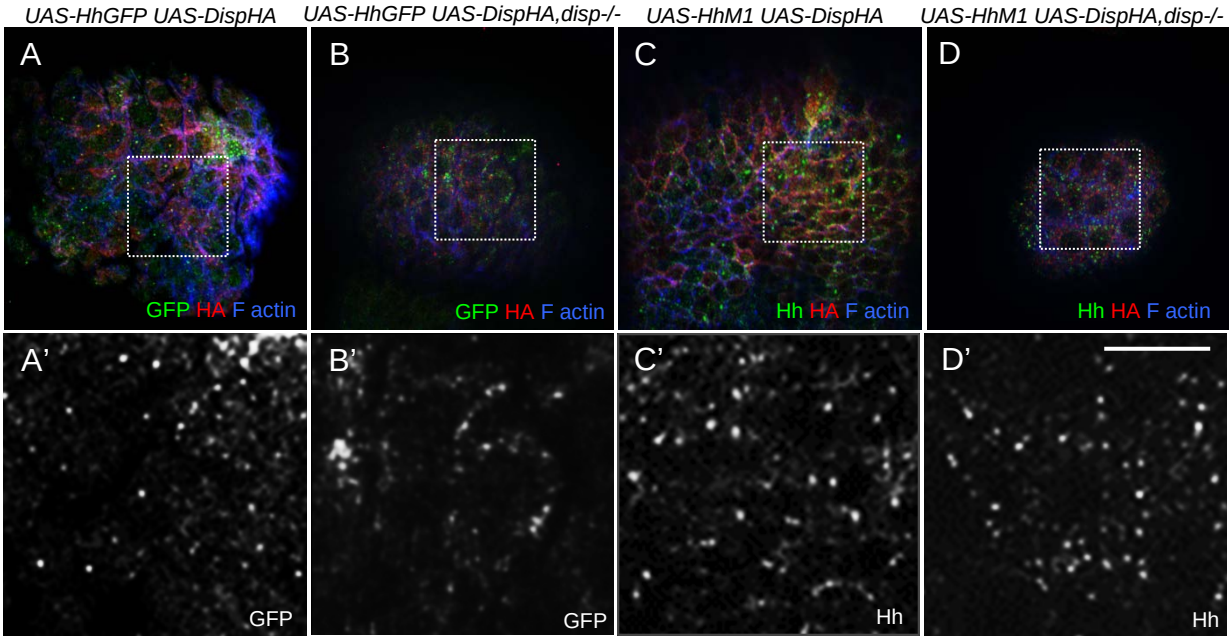

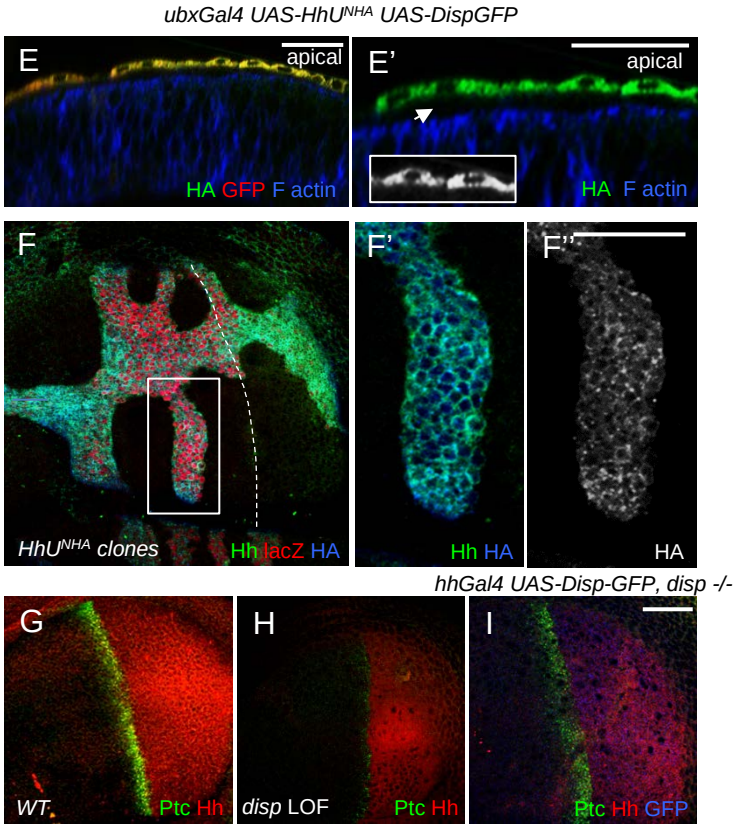

Figure S1, related to Figure 1. Live wing imaginal discs expressing UAS-YFP-Rab5^{CA} in the dorsal compartment incubated with the endocytic marker FM4-64. (A-B') Single XZ section through the posterior compartment. (B-B') Magnification of the rectangle in A depicting merged (B) and co-localization (B'). (C-C') Single XY sub-apical section of wing imaginal disc expressing YFP-Rab5^{WT} in the dorsal compartment stained with antibodies against GFP (green), Hh (red) and E-cad (blue). (C') Panel shows the single channel for Hh staining in grey. Scale bars : 20 µm. (D-F) The processing efficiency of endogenous, overexpressed Hh, or Hh-GFP was analyzed by immunoblotting the lysates of *disp-/-* mutant and *WT* wing imaginal discs, or of discs of animals expressing a Hh transgene (UAS Hh-M4) (D) or of S2 cells transfected for transient expression of UAS Hh-GFP, or untransfected S2 cells (ctrl) (E, F) using an anti-Hh (D,E), or an anti-GFP (F) antibody. The expressions of unprocessed full-length Hh (*Hh-FL*) or Hh-GFP (*Hh-FL-GFP*) and the processed form of Hh (*Hh-Np*), or Hh-GFP (*Hh-Np-GFP)* are indicated. 100 µg of protein lysates, except for WT, (50 µg), were loaded. (G) The ratio Hh-Np/Hh-FL is the mean of 4 to 6 independent experiments. The Hh-N peptide processing and levels were found to be similar in *disp* mutant and WT discs (Figure S1D, G). Note that the GFP tag, inserted near the cleavage domain of Hh (Torroja et al., 2004), could result in a less efficient processing. However, no difference in the rate of cleavage of Hh-GFP compared to endogenous Hh or to an untagged overexpressed Hh form was observed (Figure S1D-G), suggesting that the addition of the GFP tag does not affect the cleavage of the chimeric protein. Note also that the ratio Hh-Np-GFP/Hh-FL-GFP was calculated from blots revealed with the anti-GFP antibody. A *t*-test confirmed that there is no statistically significant difference for the rate of cleavage of Hh-GFP and endogenous Hh (*P*-value=0.72), or for overexpressed Hh-M4 and endogenous Hh (*P*-value = 0.77). MWM are shown on the left hand side. Individual lanes shown in each panel were from the same gel.

Figure S2, related to Figure 2. Live wing imaginal discs expressing UAS-Hh-GFP (A), UAS-Hh-N-GFP (B) or UAS-GFP-Hh-C (C) in posterior compartment incubated for 15 min with FM4-64. (A- F) Projections of 5 confocal sections 0.75 μm apart from the apical. (D-F) Magnifications of A-C. Hh-GFP (D) and Hh-N-GFP (E) are secreted into the anterior compartment (arrows). (G-O) Single XZ sections in the posterior compartment perpendicular to the D/V axis (indicated by a vertical white line in the upper panels) depicting merged (G-I) and single channels (J-O). (G) Endocytic Hh-GFP-containing vesicles co-localized with FM4-64 (circles). Note that Hh-N-GFP (H, K) is apically enriched whereas GFP-Hh-C (I, L) is cytoplasmic. (M-O) show the endocytosis of FM4-64. (P-Q') Wing imaginal disc expressing UAS-GFP-Hh-C (green) in posterior compartment stained for the Golgi marker GMAP (red). (Q) Magnification of the inset in P and co-localization (Q') of GMAP with GFP-Hh-C. A/P boundary is indicated by a dashed line. Scale bars: 20 μm.

Figure S3, related to Figure 3. (A-G') Discs after 16 hours of YFP-Rab4^{WT} (A-D'') or YFP-Rab4^{DN} (E-G') expression in the dorsal compartment stained for Hh (red and grey; A-B', G, G'), F actin (blue; A, G), YFP-Rab4^{WT} (green, A, B, D), En (blue and grey; D, D'), Ci (red and grey;D, D'') and YFP-Rab4^{WT} (green; F) for Dlg (blue; F), E-cad (red; F), YFP-Rab4^{DN} (green; F). (B-B') Single confocal XZ section in the posterior compartment across the D/V axis. (B') Hh staining is shown in gray. (C and E) Hh intensity in the posterior compartment across the D/V axis of *apGal4 tubGal80^{ts} UAS-YFP-Rab4^{WT}* (C) or *apGal4 tubGal80^{ts}UAS-YFP-Rab4^{DN}* discs (E). Note that quantification of Hh staining intensity shows a 2-fold decrease subsequent to Rab4^{DN} expression. (F) Single confocal XZ section in the posterior compartment across the D/V axis. (G-G') Extracellular Hh (Ex Hh) labeling reveals the distribution of Hh at the apical surface of the epithelium. Expression of YFP-Rab4^{DN} in dorsal cells leads to a massive accumulation of Hh as compare to ventral WT cells. (H-K') Discs overexpressing RNAi targeted against Rab4 in the dorsal compartment raised at room temperature. (H-K') The knockdown of Rab4 in the dorsal compartment decreases *dpp-lacZ* expression range (H-H'), reduces the domain of Ci stability (I-I'), but does not affect En or Ptc expression levels (J-K'), as compared to the ventral WT compartment. Quantifications in both ventral (green lines) and dorsal (red lines) compartments are plotted as a function of distance from the A/P boundary and are for the shown discs but representative of at least 6 discs from each genotype. (L-M') Discs after 24 hours of YFP-Rab5^{DN} expression in Hh producing cells at permissive (18°C) and restrictive (29°C) temperatures, stained for β-gal (L-L') or Ptc (M-M'). (N, O) Quantification of *dpp-lacZ* or Ptc staining intensity at both permissive (green lines) and restrictive (red lines) temperatures. At least 5 discs from each genotype were analyzed. Quantifications are plotted as a function of distance from the A/P boundary and are for the shown discs, but representative of all examined discs. Dotted lines label the D/V axis. The A/P border is marked by a white line. Scale bars: 20 μm**.**

Figure S4, related to Figure 4. The trafficking of Hh to the apical pole of producing cells is Disp-independent. *disp* mutant discs were analyzed by conventional (A-B') or extracellular (C-D') Hh staining. (A-B') Hh (green and grey) is strongly retained in producing cells and accumulates along the apico-basal axis. E-cad (red) marks the apical junctions. (C-D') Extracellular labeling reveals the distribution of Hh (Ex Hh) at the apical surface of the epithelium. (E-F') The lack of Disp activity does not alter the epithelial polarity of columnar cells. WT and *disp* mutant discs stained for atypical protein kinase C (aPKC, green), E-cad (red) and disc large (Dlg, blue). aPKC and E-cad are two apical markers. Dlg marks the basolateral domain. Note the identical distribution of the three proteins in both WT and *disp* mutant discs in the magnifications (E', F'). (G-I') The rescue of Disp activity restores Ptc expression in anterior cells, and permits the endocytosis of Hh-GFP in *disp* mutant posterior cells. Discs expressing Hh-GFP and Disp-HA in producing cells of *disp* mutant discs. (G-G') Panels show projection of 5 confocal sections 0.75 µm apart at the apical surface stained with HA (G-G', red and grey), Ptc (G, blue) and GFP (G, green). Note that Ptc expression domain is restored (2-3 cell rows; compare to S5H) and Hh-GFP is released and co-localizes with Ptc in the anterior compartment (inset in G). (H-I') Live discs incubated with FM4-64 (red) and chased for 15 min. (H) Single XY section and (I) single XZ section in the posterior compartment. (H'-H") are magnified images of the posterior compartment (square in H). (H'', I') show the co-localization of Hh-GFP and FM4-64. Dotted lines label the A/P boundary. The A/P border is marked by a white line. (J-L) Single XZ section of *UAS-Disp-HA; UAS-Ci-RNAi, hhGal4,tubGal80^{ts}* discs raised at 25°C (permissive temperature) up to L3 larval stage and shifted up to 29°C (restrictive temperature) for 24 hours before dissection stained for HA (green) and E-cad (red). This short induction time avoid saturation of the secretory pathway with Disp overexpression. The HA signal highlights the plasma membrane of columnar cells (C) and peripodial cells (P), including apical, lateral and basal domains.

Note accumulation of the HA signal above the E-cad apical domain in the columnar epithelium. Scale bars: 20 µm. (M-P) Electron micrographs of wing imaginal discs from (M-O) *UAS-Disp-HA, UAS-Hh-M4; hhGal4* or (P) *UAS-Disp-HA, UAS-cytoGFP ; hhGal4*. Sections were stained with antibodies to Disp-HA. The immunogold labeling of Disp-HA (15 nm) reveals Disp-HA at the plasma membrane at (M) apical microvilli (N) lateral, (O) basal and (P) sub-apical, domains. The micrograph in (P) shows a view corresponding to the white boxed area in the inset at the upper left corner. Note that the inset is at lower magnification view. L: lumen, N: nucleus. Red circles in (M) and arrows in (N-P) show examples of Disp-HA distribution at the plasma membrane.

Figure S5, related to Figure 5. Pattern of Hh and Hh-GFP particles in peripodial cells in presence or absence of endogenous Disp. (A-D) Co-expression of Hh-GFP, Disp HA (A-B) or untagged Hh (Hh-M1), Disp-HA (C-D) in peripodial cells with the *ubxGal4* driver. Single XY sections of the peripodial membrane of the indicated genotypes stained for GFP (green in A-B), HA (red), F-actin (blue in A-D), and Hh (green in C-D). (A'-D') show the single channel for GFP (grey in A', B') and Hh (grey in C', D'). Note that pattern of Hh staining is similar in all different genetic backgrounds. Also, *disp* mutant discs are much smaller compared to WT discs. The overall morphology of the discs does not allow one to observe all peripodial cells at the same focal plane. (E-E') Single XZ section of *ubxGal4 UAS-HhU^{NHA} UAS-Disp-GFP* disc stained for HA (green), GFP (red) and F-actin (blue). (E') shows the HA channel labeling the peripodial cells and the F actin channel labeling both peripodial and columnar cells. Arrow indicates the luminal space between both cell layers. No HA particles were detected within the lumen. (F-F'') Disc with clones of columnar cells expressing the HhU^{NHA} construct, labeled for Hh (green), lacZ which label the clone (red), and HA (blue). (F', F'') Magnification of the square in F. Note that no Hh-HA is detected outside the clone. (G-I) Discs of the indicated genotypes stained for Hh (red), Ptc (green) and GFP (blue). Note that *disp* mutant discs are much smaller compare to WT. Also note that the reduced Ptc expression observed in *disp* mutant disc (H) is restored in the disc expressing Disp-GFP in the posterior compartment (I). Scale bars: 20 μm.

SUPPLEMENTAL EXPERIMENTAL PROCEDURES

Drosophila stocks and reagents

The following stocks and antibodies were used: *YFP-UAS-Rab5^{WT}*, *YFP-UAS-Rab5^{DN}*, *YFP-UAS-Rab4^{WT}* (Zhang et al., 2007) were obtained from the Bloomington Stock Center. The UAS-RNAi line against Ci (Ci^{105620KK}) was from Vienna *Drosophila* RNAi Center (VDRC). *UAS-HhM4*, *UAS-HhM1* (Ingham and Fietz, 1995), *UAS-HhN-GFP* (Gorfinkiel et al., 2005), *UAS-Hh-U^{NHA}* (Chu et al., 2006), *UAS-GFP-HhC* (a chimera with the Hh-N peptide replaced with GFP) was from S. Eaton), *UAS-Disp-GFP* (a Disp C terminal fusion with GFP, this study), *UAS-cytoGFP*.

Antibodies were used at the following dilutions: rabbit polyclonal anti-aPKC (Santa Cruz), 1/500; mouse DLG1 monoclonal ant-Dlg (DSHB), 1/100; rabbit anti-GMAP (Friggi-Grelin et al., 2006) 1/500.

Western blots

WT or *disp^{377}* imaginal discs or heads from L3 *hhGal4*, *UAS-Hh-M4* were dissected in ice-cold PBS. S2 cells were transiently transfected or not with UAS-Hh-GFP. Tissues and cells were homogenized for 30 min on ice in lysis buffer (150 mMNaCl, 50 mM Tris, 1% Triton X-100, 0.5% sodium deoxycholate, 0.1% SDS, pH 7.5) supplemented with a protease inhibitor mixture. The proteins were separated by SDS-PAGE and analyzed by immunoblotting with rabbit "Calvados" polyclonal anti-Hh antibody (Gallet et al., 2003) or mouse anti-α-tubulin monoclonal antibody (Sigma), followed by anti-rabbit and anti-mouse HRP (1:10000). Protein detection by enhanced chemiluminescence was realized by Fuji3000 camera.

Immunoelectron Microscopy (IEM)

IEM was carried out according to the Tokuyasu method. Briefly, samples were fixed in phosphate buffer containing 2% paraformaldehyde and 0.2% glutaraldehyde, embedded in gelatin, cryoprotected in sucrose and frozen in liquid nitrogen. 80nm-thick cryosections were then incubated with a mouse anti-HA antibody (16B12, Covance, 1:300) that was recognized by a rabbit anti-mouse antibody (Rockland, 1:250) and protein-A gold-conjugates (15 nm, purchased from the Cell Microscopy Center, Department of Cell Biology, Utrecht University, The Netherlands). Cryosections were observed at 80 kV with a 120 kV JEOL JEM-1400 electron microscope and digital acquisitions made with a numeric MORADA camera (Olympus SIS). Cryosectioning and microscope observation was performed at the CCMA EM core facility (Université Nice Sophia Antipolis).

SUPPLEMENTAL REFERENCES

Callejo, A., Torroja, C., Quijada, L., and Guerrero, I. (2006). Hedgehog lipid modifications are required for Hedgehog stabilization in the extracellular matrix. Dev. Camb. Engl. *133*, 471–483.

Chu, T., Chiu, M., Zhang, E., and Kunes, S. (2006). A C-terminal motif targets Hedgehog to axons, coordinating assembly of the Drosophila eye and brain. Dev. Cell *10*, 635–646.

Friggi-Grelin, F., Rabouille, C.and Therond, P. (2006). The cis-Golgi Drosophila GMAP has a role in anterograde transport and Golgi organization in vivo, similar to its mammalian ortholog in tissue culture cells. Eur. J. Cell Biol. *85*, 1155–1166.

Gorfinkiel, N., Sierre, J., CAllejo, A., Ibanez, C., and Guerrero, I. (2005). The Drosophila ortholog of the human Wnt inhibitor factor Shifted controls the diffusion of the lipid-modified Hedgehog. Dev. Cell *8*, 241-253.

Ingham, P.W and Fietz, M.J. (1995). Quantitative effects of hedgehog and decapentaplegic activity on the patterning of Drosophila wing. Curr. Biol. CB *5*, 432–440.